

PLOS ONE

STRUCTURAL AND DYNAMICS EVIDENCE FOR SCAFFOLD ASYMMETRIC FLEXIBILITY OF THE HUMAN TRANSTHYRETIN TETRAMER

--Manuscript Draft--

Manuscript Number:	PONE-D-17-29675R1
Article Type:	Research Article
Full Title:	STRUCTURAL AND DYNAMICS EVIDENCE FOR SCAFFOLD ASYMMETRIC FLEXIBILITY OF THE HUMAN TRANSTHYRETIN TETRAMER
Short Title:	ASYMMETRIC FLEXIBILITY OF THE HUMAN TRANSTHYRETIN TETRAMER
Corresponding Author:	Giuseppe Zanotti University of Padua Padova, PD ITALY
Keywords:	Transthyretin; TTR; tetrameric proteins; ligand; normal-mode analysis; flexibility.
Abstract:	<p>The molecular symmetry of multimeric proteins is generally determined by using X-ray diffraction techniques, so that the basic question as to whether this symmetry is perfectly preserved for the same protein in solution remains open. In this work, human transthyretin (TTR), a homotetrameric plasma transport protein with two binding sites for the thyroid hormone thyroxine (T4), is considered as a case study. Based on the crystal structure of the TTR tetramer, a hypothetical D2 symmetry is inferred for the protein in solution, whose functional behavior reveals the presence of two markedly different Kd values for the two T4 binding sites. The latter property has been ascribed to an as yet uncharacterized negative binding cooperativity. A triple mutant form of human TTR (F87M/L110M/S117E TTR), which is monomeric in solution, crystallizes as a tetrameric protein and its structure has been determined. The exam of this and several other crystal forms of human TTR suggests that the TTR scaffold possesses a significant structural flexibility. In addition, TTR tetramer dynamics simulated using normal modes analysis exposes asymmetric vibrational patterns on both dimers and thermal fluctuations reveal small differences in size and flexibility for ligand cavities at each dimer-dimer interface. Such small structural differences between monomers can lead to significant functional differences on the TTR tetramer dynamics, a feature that may explain the functional heterogeneity of the T4 binding sites, which is partially overshadowed by the crystal state.</p>
Order of Authors:	<p>Giuseppe Zanotti</p> <p>Francesca Vallese</p> <p>Alberto Ferrari</p> <p>Ilaria Menozzi</p> <p>Tadeo E Saldaño</p> <p>Paola Berto</p> <p>Sebastian Fernandex-Alberti</p> <p>Rodolfo Berni</p>
Opposed Reviewers:	
Response to Reviewers:	<p>Padua, October 20th, 2017</p> <p>Dear Editor,</p> <p>I am submitting the manuscript entitled "STRUCTURAL AND DYNAMICS EVIDENCE FOR SCAFFOLD ASYMMETRIC FLEXIBILITY OF THE HUMAN TRANSTHYRETIN TETRAMER" revised according to the reviewers' suggestions. I hope that in the present form the paper is acceptable for publication in PlosOne.</p> <p>A point-by-point reply to all comments is included.</p>

	<p>Thank you in advance for considering this manuscript.</p> <p>Sincerely,</p> <p>Prof. Giuseppe Zanotti Department of Biomedical Sciences University of Padua</p>
Additional Information:	
Question	Response
<p>Financial Disclosure</p> <p>Please describe all sources of funding that have supported your work. This information is required for submission and will be published with your article, should it be accepted. A complete funding statement should do the following:</p> <p>Include grant numbers and the URLs of any funder's website. Use the full name, not acronyms, of funding institutions, and use initials to identify authors who received the funding.</p> <p>Describe the role of any sponsors or funders in the study design, data collection and analysis, decision to publish, or preparation of the manuscript. If the funders had no role in any of the above, include this sentence at the end of your statement: "<i>The funders had no role in study design, data collection and analysis, decision to publish, or preparation of the manuscript.</i>"</p> <p>However, if the study was unfunded, please provide a statement that clearly indicates this, for example: "<i>The author(s) received no specific funding for this work.</i>"</p> <p>* typeset</p>	<p>This work received financial support from: Universities of Padua and Parma, Italy; MIUR (Ministero Istruzione Universita` Ricerca, Italy) PRIN (Progetti di Rilevante Interesse Nazionale) Project 2012A7LMS3_002.</p>
<p>Competing Interests</p> <p>You are responsible for recognizing and disclosing on behalf of all authors any competing interest that could be perceived to bias their work, acknowledging all financial support and any other relevant financial or non-financial competing interests.</p> <p>Do any authors of this manuscript have</p>	<p>The authors have declared that no competing interests exist</p>

<p>competing interests (as described in the PLOS Policy on Declaration and Evaluation of Competing Interests)?</p> <p>If yes, please provide details about any and all competing interests in the box below. Your response should begin with this statement: <i>I have read the journal's policy and the authors of this manuscript have the following competing interests:</i></p> <p>If no authors have any competing interests to declare, please enter this statement in the box: <i>"The authors have declared that no competing interests exist."</i></p> <p>* typeset</p>	
<p>Ethics Statement</p> <p>You must provide an ethics statement if your study involved human participants, specimens or tissue samples, or vertebrate animals, embryos or tissues. All information entered here should also be included in the Methods section of your manuscript. Please write "N/A" if your study does not require an ethics statement.</p> <p>Human Subject Research (involved human participants and/or tissue)</p> <p>All research involving human participants must have been approved by the authors' Institutional Review Board (IRB) or an equivalent committee, and all clinical investigation must have been conducted according to the principles expressed in the Declaration of Helsinki. Informed consent, written or oral, should also have been obtained from the participants. If no consent was given, the reason must be explained (e.g. the data were analyzed anonymously) and reported. The form of consent (written/oral), or reason for lack of consent, should be indicated in the Methods section of your manuscript.</p> <p>Please enter the name of the IRB or Ethics Committee that approved this study in the space below. Include the approval number and/or a statement indicating</p>	<p>N/A</p>

approval of this research.

Animal Research (involved vertebrate animals, embryos or tissues)

All animal work must have been conducted according to relevant national and international guidelines. If your study involved non-human primates, you must provide details regarding animal welfare and steps taken to ameliorate suffering; this is in accordance with the recommendations of the Weatherall report, "[The use of non-human primates in research.](#)" The relevant guidelines followed and the committee that approved the study should be identified in the ethics statement.

If anesthesia, euthanasia or any kind of animal sacrifice is part of the study, please include briefly in your statement which substances and/or methods were applied.

Please enter the name of your Institutional Animal Care and Use Committee (IACUC) or other relevant ethics board, and indicate whether they approved this research or granted a formal waiver of ethical approval. Also include an approval number if one was obtained.

Field Permit

Please indicate the name of the institution or the relevant body that granted permission.

Data Availability

PLOS journals require authors to make all data underlying the findings described in their manuscript fully available, without restriction and from the time of publication, with only rare exceptions to address legal and ethical concerns (see the [PLOS Data Policy](#) and [FAQ](#) for further details). When submitting a manuscript, authors must provide a Data Availability Statement that describes where the data underlying their manuscript can be found.

Your answers to the following constitute your statement about data availability and will be included with the article in the event of publication. **Please note that**

Yes - all data are fully available without restriction

<p>simply stating 'data available on request from the author' is not acceptable. <i>If, however, your data are only available upon request from the author(s), you must answer "No" to the first question below, and explain your exceptional situation in the text box provided.</i></p> <p>Do the authors confirm that all data underlying the findings described in their manuscript are fully available without restriction?</p>	
<p>Please describe where your data may be found, writing in full sentences. Your answers should be entered into the box below and will be published in the form you provide them, if your manuscript is accepted. If you are copying our sample text below, please ensure you replace any instances of XXX with the appropriate details.</p> <p>If your data are all contained within the paper and/or Supporting Information files, please state this in your answer below. For example, "All relevant data are within the paper and its Supporting Information files."</p> <p>If your data are held or will be held in a public repository, include URLs, accession numbers or DOIs. For example, "All XXX files are available from the XXX database (accession number(s) XXX, XXX)." If this information will only be available after acceptance, please indicate this by ticking the box below. If neither of these applies but you are able to provide details of access elsewhere, with or without limitations, please do so in the box below. For example:</p> <p>"Data are available from the XXX Institutional Data Access / Ethics Committee for researchers who meet the criteria for access to confidential data."</p> <p>"Data are from the XXX study whose authors may be contacted at XXX."</p> <p>* typeset</p>	<p>Data area available from the PDB with the ID code 5OQ0</p>
<p>Additional data availability information:</p>	<p>Tick here if the URLs/accession numbers/DOIs will be available only after acceptance of the manuscript for publication so that we can ensure their inclusion before publication.</p>

DIPARTIMENTO DI SCIENZE BIOMEDICHE - DSB

DEPARTMENT OF BIOMEDICAL SCIENCES

Via Ugo Bassi 58/B

35131 Padova

Italy

www.biomed.unipd.it



**UNIVERSITÀ
DEGLI STUDI
DI PADOVA**

Padua, October 20th, 2017

Dear Editor,

I am submitting the manuscript entitled “STRUCTURAL AND DYNAMICS EVIDENCE FOR SCAFFOLD ASYMMETRIC FLEXIBILITY OF THE HUMAN TRANSTHYRETIN TETRAMER” revised according to the reviewers’ suggestions. I hope that in the present form the paper is acceptable for publication in *PlosOne*.

A point-by-point reply to all comments is included.

Thank you in advance for considering this manuscript.

Sincerely,

Prof. Giuseppe Zanotti
Department of Biomedical Sciences
University of Padua

A handwritten signature in blue ink, appearing to read 'G. Zanotti'.

1

2 **STRUCTURAL AND DYNAMICS EVIDENCE FOR SCAFFOLD**

3 **ASYMMETRIC FLEXIBILITY OF THE HUMAN TRANSTHYRETIN**

4 **TETRAMER**

5

6

7 Giuseppe Zanotti ^{1*}, Francesca Vallese ¹, Alberto Ferrari ², Ilaria Menozzi ², Tadeo E. Saldaño³,

8 Paola Berto¹, Sebastian Fernandez-Alberti³, and Rodolfo Berni ²

9

10 ¹ Department of Biomedical Sciences, University of Padua, Padua, Italy

11 ² Department of Chemical Sciences, Life Sciences and Environmental Sustainability, University of

12 Parma, Parma, Italy

13 ³ Universidad Nacional de Quilmes/CONICET, Bernal, Argentina

14

15

16 * Corresponding author

17 E-mail: giuseppe.zanotti@unipd.it

18

19 **Abstract**

20 The molecular symmetry of multimeric proteins is generally determined by using X-ray
21 diffraction techniques, so that the basic question as to whether this symmetry is perfectly preserved
22 for the same protein in solution remains open. In this work, human transthyretin (TTR), a
23 homotetrameric plasma transport protein with two binding sites for the thyroid hormone thyroxine
24 (T4), is considered as a case study. Based on the crystal structure of the TTR tetramer, a
25 hypothetical D2 symmetry is inferred for the protein in solution, whose functional behavior reveals
26 the presence of two markedly different K_d values for the two T4 binding sites. The latter property
27 has been ascribed to an as yet uncharacterized negative binding cooperativity. A triple mutant form
28 of human TTR (F87M/L110M/S117E TTR), which is monomeric in solution, crystallizes as a
29 tetrameric protein and its structure has been determined. The exam of this and several other crystal
30 forms of human TTR suggests that the TTR scaffold possesses a significant structural flexibility. In
31 addition, TTR tetramer dynamics simulated using normal modes analysis exposes asymmetric
32 vibrational patterns on both dimers and thermal fluctuations reveal small differences in size and
33 flexibility for ligand cavities at each dimer-dimer interface. Such small structural differences
34 between monomers can lead to significant functional differences on the TTR tetramer dynamics, a
35 feature that may explain the functional heterogeneity of the T4 binding sites, which is partially
36 overshadowed by the crystal state.

37

38 **Introduction**

39 Human transthyretin (TTR) is a homotetrameric protein involved in the transport in
40 extracellular fluids of thyroxine (T4) and in the co-transport of vitamin A, by forming a
41 macromolecular complex with plasma retinol-binding protein [1,2]. Its structure was determined in
42 the late seventies and is now known at high resolution [3,4]. The TTR monomer is composed of two
43 four-stranded anti-parallel β -sheets and a short α -helix; two monomers are held together to form a

44 very stable dimer through a net of H-bond interactions involving the two edge β -strands H and F, in
45 such a way that a pseudo-continuous eight-stranded β -sandwich is generated, in which H and F β -
46 strands from each monomer in the dimer are connected to each other by main-chain H-bonds and
47 H-bonded water molecules. Structurally, the TTR tetramer is a dimer of dimers, in which the two
48 dimers associate, interacting mostly through hydrophobic contacts between residues of the AB and
49 GH loops. The assembly of the four identical subunits in TTR is highly symmetrical, being
50 characterized by 222 symmetry. A long channel, coincident with one of the 2-fold symmetry axes,
51 transverses the whole protein and harbors two T4 binding sites at the dimer-dimer interface.

52 Despite the presence in the TTR tetramer of two identical binding sites, which are both
53 occupied in the crystal with roughly similar mode of binding by T4 [1], its binding in solution is
54 characterized by a strong negative cooperativity, with about two order of magnitude difference in
55 the K_d values for the first and second T4 bound to TTR [5]. Recently, additional evidence for TTR
56 binding site heterogeneity both in solution, using the polyphenol resveratrol as a fluorescent ligand
57 [6], and in the crystal [7], has been obtained. More than 240 crystal structures of TTR in complex
58 with a variety of chemically different ligands, whose binding often exhibits negative cooperativity,
59 are present to date in the Protein Data Bank. Nevertheless, the molecular basis of the cooperative
60 behavior and of the heterogeneity of T4 binding sites remains to be clarified.

61 Human TTR and a number of its mutant forms have been associated with amyloid diseases
62 [8]. Amyloidoses are generated by the misfolding, misassembly and pathological aggregation of
63 several proteins, among which human TTR represents a remarkable example. Evidence has been
64 obtained by JW Kelly and coworkers to indicate that the rate-limiting dissociation of the native
65 tetrameric state into monomers, followed by misfolding of TTR monomers and their downhill
66 polymerization, leads to the formation of protein aggregates *in vitro*, and presumably *in vivo* ([9],
67 and references therein). Following these observations, the properties of a large number of TTR
68 ligands have been investigated in prospect of their use as drugs effective in the therapy of TTR

69 amyloidosis. In fact, T4 and other specific TTR ligands are able to stabilize the TTR tetramer and to
70 inhibit protein aggregation by occupying the T4 binding sites and establishing interactions that
71 connect the couple of subunits that form each binding site [9] [10] [11] [12]. Interestingly, it has
72 been inferred that the degree of negative binding cooperativity of a ligand is inversely related to its
73 ability to saturate and stabilize the TTR tetramer, so that features related to binding cooperativity
74 may also be relevant with regard to the anti-amyloidogenic potential of ligands [12].

75 Consistent with the observation that monomeric TTR may represent a key species along the
76 pathway of TTR amyloidogenesis, two mutations (F87M-L110M) able to induce the dissociation of
77 TTR into monomers were found to drastically accelerate protein aggregation *in vitro* [13]. An
78 additional mutation (S117E) has been introduced here in the sequence of the double TTR mutant, to
79 obtain a triple mutant, which is characterized by a stronger tendency to dissociate into the
80 monomeric state in solution, in comparison with the double mutant. However, crystal packing in the
81 presence of high protein concentration led to the formation of the TTR tetramer, whose structure
82 has been determined. Here, we report on the comparison of structural features of the triple
83 F87M/L110M/S117E TTR mutant and of other, previously characterized, forms of human TTR,
84 both wild type and mutant forms, crystallized in different space groups. Our data provide evidence
85 for a significant structural flexibility and asymmetric dynamics of the scaffold of the TTR tetramer,
86 a feature that leads to asymmetric functional properties of this protein in solution, such as those
87 associated with its putative cooperative behavior.

88 **Materials and methods**

89 **Crystallization and structure determination**

90 Recombinant mutant forms (F87M/L110M and F87M/L110M/S117E) of human TTR were
91 prepared by site-directed mutagenesis essentially as described [14]. Crystals of the triple
92 (F87M/L110M/S117E) TTR mutant were grown using the hanging-drop vapor diffusion method. 2

93 μ l of protein (7.3 mg/ml) solution in 50mM Tris-HCl (pH 8.0), 1 M ammonium sulfate, were
94 equilibrated against a well solution (100 μ l) containing 0.1 M sodium phosphate (pH 7.5), 2.2 M
95 ammonium sulfate. Single crystals of approximate size 0.02 mm in the longest dimension were
96 obtained in about a week of incubation at room temperature. 1500 images with an oscillation of
97 0.15° each were collected at the ID30B beamline of European Synchrotron Radiation Facility
98 (ESRF, Grenoble, France) for a total exposure time of 55.5 s. The crystal belongs to the space group
99 I222, with one monomer in the asymmetric unit. Datasets were processed with the software XDS
100 [15] and scaled with Scala [16] contained in the CCP4 suite [17]. The space group is I222, with one
101 monomer per asymmetric unit ($V_M = 2.05$, estimated solvent content 40%). The physiological
102 tetramer is generated through the crystallographic two-fold axes. The structure was solved by
103 molecular replacement using as a template one monomer of wild-type TTR in the P2₁2₁2 space
104 group (PDB ID 4W00, [7]) and refined using the package Phenix [18]. In the last cycles, TLS
105 refinement was applied. Map visualization and manual adjustment of the models were performed
106 using the Coot graphic interface [19]. Statistics on data collection and refinement are reported in
107 Table 1.

108

109 **Table 1. Data collection and refinement statistics.**

Data set	TTR I222
Wavelength (Å)	0.973186
Cell dimensions <i>a</i> , <i>b</i> , <i>c</i> (Å)	42.25 67.045 83.57
Resolution (Å)	52.29 - 1.94 (2.01 - 1.94)*
Reflections (unique)	8849 (687)
R_{merge}	0.073 (0.916)
R_{pim}	0.030 (0.514)
$\langle I/\sigma(I) \rangle$	13.0 (1.6)

<CC(1/2)>	0.998 (0.396)
Completeness (%)	97.4 (80.5)
Redundancy	7.2 (4.8)
Refinement	
No. reflections	8841
$R_{\text{work}} / R_{\text{free}}$	0.2296 (0.310) / 0.2671(0.347)
No. protein / solvent atoms	896 / 25
R.m.s. deviations	
Bond lengths (Å)	0.008
Bond angles (°)	0.944
Ramachandran plot	
Favored /outliers (%)	96.5 / 0.0
Rotamer outliers (%) / C β - outliers	2.1 / 0
Overall MolProbity score**	1.54

110

111 * Numbers in parentheses refer to the last resolution shell

112 ** See reference [35]

113 **Normal modes analysis**

114 Normal mode analysis has been calculated using the Elastic Network Model (ENM) [20] [21] [22]

115 [23] [24]. The model represents a protein structure as a network of N nodes. Herein, we have

116 considered as nodes the atoms of protein backbone, C β and the center of mass of side chains.

117 Springs connect each node to their neighbors within a cut-off distance $r_c = 7\text{\AA}$. The resulted

118 potential energy is defined, according to [20] [25] [26], as

119
$$E(\mathbf{r}_i, \mathbf{r}_j) = \frac{1}{2}k_{ij}(|\mathbf{r}_{ij}| - |\mathbf{r}_{ij}^0|)^2$$

120 where $\mathbf{r}_{ij} \equiv \mathbf{r}_i - \mathbf{r}_j$ is the vector connecting nodes i and j , and the zero superscript indicates the
121 position at the crystallographic structure. The value of the force constant k_{ij} varies according to the
122 type of interaction between nodes i and j [27] [28]. Normal modes are obtained as a set of
123 eigenvectors $\{\mathbf{Q}_i\}_{i=1, 3N}$ of the Hessian matrix, defined as the matrix of second-order partial
124 derivatives of the potential energy. Each \mathbf{Q}_i is a $3N$ vector whose elements $\{c_i^j\}_{j=1, 3N}$ represent the
125 relative displacements of Cartesian coordinates of each j^{th} residue. Therefore, for each normal mode
126 \mathbf{Q}_i , the fraction of relative displacements of residues belonging to subunit A-A' can be calculated
127 as $\sum_{j \in A-A'} (c_i^j)^2$.

128 **Set of structures representing thermal fluctuations**

129 A set of 1000 structures representing thermal distortions has been generated from the original X-ray
130 (PDB ID 1F41) uncomplexed TTR structure by randomly displacements in the direction of each
131 normal modes i within the range $[-A_i; A_i]$, being A_i (\AA) the corresponding amplitude of the mode at
132 room temperature

$$133 \quad A_i = \left(\frac{2k_B T}{\lambda_i} \right)^{1/2}$$

134 where k_B is the Boltzmann constant and T is the absolute temperature (300K). λ_i corresponds to the
135 eigenvalue associated to the i^{th} normal mode scaled in order to best fit the theoretical residue
136 fluctuations with the corresponding experimental temperature factors. The average root mean
137 square difference between structures was ~ 0.4 .

138

139 **Results**

140 **Crystal structure of the F87M/L110M/S117E TTR mutant form**

141 Out of a total of 240 human TTR structures present in the Protein Data Bank, 218 structures,
142 including those of several TTR mutant forms and TTR-ligand complexes, belong to the

143 orthorhombic space group $P2_12_12$. In such structures a dimer is present in the asymmetric unit, and
144 the second dimer is generated by symmetry, owing to the two-fold crystallographic axis coincident
145 with the central channel in the TTR tetramer. The resulting tetramer present in such crystal can
146 deviate from the ideal 222 symmetry, owing to the fact that only one of the two-fold axes is
147 coincident with the crystallographic one. On the contrary, crystals of the structure presented here
148 for the triple F87M/L110M/S117E TTR mutant belong to space group $I222$, where only one
149 monomer is present in the asymmetric unit, and the tetramer is generated by the crystallographic
150 symmetry (**Fig 1**). At variance with the structures obtained from crystals belonging to the space
151 group $P2_12_12$, in the centered $I222$ space group, the molecular symmetry of the protein is fully
152 coincident with the crystallographic one. The other known structure in this crystal form is that of
153 the V122I TTR mutant in complex with tolcapone [12]. In both cases the tetramer generated by the
154 crystallographic axes is equivalent to that of the already known structure of TTR [4].

155

156 **Fig 1. Cartoon view of the TTR tetramer.** The two black lines on the plane of the page and the
157 black dot in the center correspond to molecular two-fold axes. In the case of the $P2_12_12$ space
158 group, the central dot corresponds to the crystallographic two-fold axis, perpendicular to the plane
159 of the page. In the $I222$ space group, all three axes are crystallographic elements of symmetry.
160 Chains are all identical, but they are labelled A and B or and A, B, C and D when a dimer or a
161 tetramer is present in the asymmetric unit, respectively.

162

163 The final model in the $I222$ space group is essentially the same observed in the case of the
164 $P2_12_12$ crystal form. In fact, the r.m.s.d. for the superposition of 114 equivalent $C\alpha$ atoms of the
165 monomer of the triple F87M/L110M/S117E TTR mutant with those of a representative wt TTR
166 structure (PDB 1F41 [4]) is 0.52 Å for monomer A and 0.78 Å for monomer B. Similar low r.m.s.d.
167 for the superposition of the wt TTR structure (PDB 1F41) to TTR crystallized in other space groups
168 are also found: 0.39 Å for the V122I TTR mutant in complex with tolcapone (PDB 5A6I [12]);

169 0.45 Å for the double F87M-L110M TTR mutant (PDB 1GKO [13]); 0.60 Å for wt TTR in complex
170 with 4-hydroxy-chalcone (PDB 5EZF [29]); 0.74 Å for the monoclinic C2 crystals of the L55P TTR
171 mutant (PDB 5TTR [30]); 0.64 Å for the wt TTR monoclinic P2₁ crystals (PDB 1ICT [31]).

172 The triple F87M/L110M/S117E TTR mutant ~~in solution~~ is characterized by a high
173 propensity to keep a monomeric state in solution, greater than that of the double F87M/L110M TTR
174 mutant, even in the presence of the strong fibrillogenesis inhibitor tafamidis [10] (**Fig S1**). The main
175 reason for the pronounced tetramer destabilization could be due to the presence of the side chains of
176 two pairs of Glu117, one towards the other, in the inner part of the cavity for each couple of
177 subunits (A-A' and B-B'). The distances between the two Oε1 and Oε2 of Glu117 residues of
178 subunits A and A' are in fact 5.15 Å and 5.06 Å, respectively, thereby generating a strong
179 electrostatic repulsion, provided that they are negatively charged. On the other hand, the distance
180 between two Oε2 atoms of Glu117 of subunits A and B' (and of B and A') is 2.79 Å in the crystal,
181 which is consistent with the formation of H bond interactions between each couple of the above
182 subunits and, consequently, with the presence of tetrameric TTR in the crystal. The different
183 aggregation state found for the protein in the crystal and in solution may depend on contacts
184 between subunits and dimers induced by crystal lattice constraints and on differences in pKa values
185 of the carboxylic groups of Glu117 residues of the proteins in the two physical states.

186

187 **Relationships between monomers for different TTR crystal forms**

188 To analyze the structural differences induced by the presence or absence of the
189 crystallographic symmetry for structures determined from crystals belonging to different space
190 groups, we have compared several TTR structures, as follows: the triple F87M/L110M/S117E TTR
191 mutant; the wild type TTR form (PDB 1F41 [4]), as representative of a high-resolution structure of
192 wild type TTR; the double F87M/L110M TTR mutant, which crystallizes in the P2₁2₁2₁ space
193 group with a tetramer in the asymmetric unit (PDB 1GKO, [13]); the V122I TTR mutant in

194 complex with tolcapone (PDB 5A6I, [12]), the only other TTR structure containing a single
195 monomer in the asymmetric unit; the wild type TTR in complex with 4-hydroxy-chalcone (PDB
196 5EZP, [29]), which crystallizes in the $P3_1$ space group, with two tetramers in the asymmetric unit.
197 In the latter case, only one tetramer was considered in the comparison. Data for the structure of the
198 L55P TTR mutant (PDB 5TTR, [30]), crystallized in space group C2 with one tetramer and two
199 dimers in the asymmetric unit, are not reported in detail, but the general behavior is the same, as
200 established for the other TTR crystal forms.

201

202

203 **Fig. 2 Comparison of the structures of TTR from different crystal forms.** Superposition of $C\alpha$
204 chain traces of (I) triple F87M/L110M/S117E TTR mutant to 1F41 structure, (II) triple TTR mutant
205 to 56A1 structure, (III) triple TTR mutant to double TTR mutant 1GKO structure, (IV) triple TTR
206 mutant to 5EZP structure, (V) 1F41 to 56A1 structures. In all cases, only monomers A were
207 superimposed. The four monomers of the TTR triple mutant are shown in different colors, the
208 others in the same color.

209

210 If the $C\alpha$ atoms of one subunit, say A, are superimposed, we can visualize the differences in
211 the position of the other subunits in relationships with that of subunit A for different crystal
212 structures/space groups (**Fig 2**). In Table 2, a more quantitative estimate of the differences is given
213 by the measure of the distances between equivalent $C\alpha$ atoms for subunits B, A' and B'. An
214 analysis of these distances indicates that by superimposing monomers A of TTR tetramers from
215 crystals belonging to different space groups, monomers B, A' and B' are displaced apparently in a
216 random way. This indicates that taking monomer A as reference, the other monomers present a
217 slightly different orientation for different crystal forms. For example, with the crystallographic two-
218 fold axis of space group $P2_12_12$ running vertical in the page, by comparing the structures of the
219 triple F87M/L110M/S117E TTR mutant and of wild type TTR (PDB 1F41), monomers B'

220 superimpose quite well, whilst B and A' are significantly displaced (**Fig 2, panel I**). On the
 221 contrary, in the superposition of 1F41 and 5A6I structures A and B are nearly coincident, while the
 222 positions of A' and B' diverge significantly (**Fig 2, panel IV**).

223

224 **Table 2. Interatomic distances between equivalent atoms in different TTR tetramers.**

	87/110/117 TTR mutant – wild type TTR (1F41) *	87/110/117 TTR mutant - V122I TTR mutant (5A6I)	87/110/117 TTR mutant - 87/110 TTR mutant (1GKO)	1F41 wild typeTTR - V122I TTR mutant (5A6I)	87/110/117 TTR mutant - 4-hydroxy- chalcone - TTR complex(5EZP)
Thr 96 B	2.44	1.71	2.02	0.98	2.37
Thr 96 C (A')	1.29	1.97	2.08	1.73	1.15
Thr 96 D (B')	2.38	1.42	2.58	2.69	2.36
Leu55 B	1.77	2.26	2.13	0.77	1.06
Leu55 C (A')	1.86	1.56	1.45	0.47	0.80
Leu55 D (B')	2.27	1.52	2.67	2.11	1.90
Ser85 B	3.52	0.96	0.99	3.03	2.37
Ser85 C (A')	3.42	2.39	3.27	2.65	2.26
Ser85 D (B')	3.98	2.83	2.48	1.81	2.68

225 Distances (in Å) between C α atoms for pair of proteins in subunits B, C and D, after superimposing
 226 subunit A of the models. Residues of monomer A are not indicated, since they are practically
 227 coincident.

228 *C and D labels correspond to A' and B' in the P₂₁2₁2 space group, i.e. the crystallographic two-
 229 fold axis superimposes A' to A and B' to B.

230

231 In turn, this situation has consequences on the size of TTR binding cavities. To give an
 232 indication of the size of each of the two cavities, distances between corresponding C α atoms of
 233 monomers A – A' and B – B' (i.e. the couples of subunits that line the two T4 binding cavities) are
 234 compared in **Table 3**. Interestingly, these distances are in some cases quite different from one
 235 structure to the other, a fact possibly due to real differences in the size of the cavity (also
 236 considering that two of the reported structures are those of TTR mutant forms). However, such
 237 differences could also partially reflect the slightly different cell parameters of the structures
 238 considered. More relevant, since not affected by systematic errors, is the internal comparison
 239 between the same distance between residues in the cavities formed by monomers A –A' and B – B' .
 240 When only a TTR monomer is present in the asymmetric unit, i.e. a perfect tetramer is present in
 241 the crystal, the two cavities are identical by symmetry; in the other cases, where a dimer or an entire
 242 tetramer is present in the asymmetric unit, the two may differ in size. As expected, distances
 243 between residues close to the center of the tetramer are less affected by the rotation of one monomer
 244 relative to the other, whilst those far from the center of the tetramer present larger differences.
 245 These differences are very small for wild type TTR (PDB 1F41), in which one dimer is present in
 246 the crystal asymmetric unit, and definitely larger in cases where an entire tetramer is present in the
 247 asymmetric unit, as for the 4-hydroxy-chalcone in complex with TTR and for the double
 248 F87M/L110M TTR mutant. In the latter, the most astonishing difference is represented by residues
 249 T119, for which there are more than 4Å differences in the distances between A - A' and B - B' (the
 250 latter are labeled A – C and B – D in the original structure, since there is a tetramer in the
 251 asymmetric unit). It must be considered anyhow that all the examined structures have been
 252 determined at different resolutions.

253

254 **Table 3. Distances (in Å) between C α atoms of subunits A and C (or A') and B and D (or B').**

	87/110/117	87/110 TTR	V122I TTR	wild type TTR	4-hydroxy-
--	------------	------------	-----------	---------------	------------

	TTR mutant A – A'	mutant (1GKO) A – A' / B – B'	mutant (5A6I) A – A'	(1F41) A – A' / B – B'	chalcone - TTR complex (5EZP) A – A' / B – B'
S(E)117	9.67	9.54 / 9.92	8.75	9.36 / 9.30 (9.39)	9.83 / 9.86
T119	14.17	15.19 / 11.63	13.45	13.30 / 13.17 (13.35)	13.47 / 13.77
A108	11.70	10.45 / 11.82	11.98	11.84 / 11.86	11.56 / 11.73
K15	13.81	12.65 / 14.57	14.14	13.85 / 13.88	13.63 / 13.93
T106	17.72	17.82 / 16.27	17.59	17.94 / 17.80	17.84 / 18.30

255 In the case of the presence of a perfect tetramer in the asymmetric unit only one distance is
256 reported.

257

258 **Normal mode analysis of the TTR tetramer**

259 Using normal mode analysis, we have analyzed differences in the flexibilities of residues in the
260 couples of subunits A-A' and B-B', which form the two binding sites at the dimer-dimer interface
261 in the TTR tetramer. For this purpose, the fraction of relative displacements involving C α atoms of
262 subunit A-A' has been calculated for each normal mode of the wild type ligand-free TTR tetramer
263 (PDB 1F41). The distribution of these values is depicted in **Fig 3**. The peak at values of ~1
264 corresponds to normal modes entirely localized on the A-A' moiety, while normal modes localized
265 on the B-B' moiety are represented by the peak at ~0. The maximum at ~0.5 indicates that most of
266 normal modes are equally distributed between both moieties. Nevertheless, the distribution is not
267 completely symmetric.

268

269

270 **Fig 3. Displacement of subunits.** Distribution of fraction of relative displacements involving $C\alpha$
271 atoms of subunit A-A' evaluated on each normal mode of wild-type ligand-free TTR tetramer
272 normal modes.

273

274 In order to analyze functional aspects of the structural and dynamics asymmetries between
275 subunits A-A' and B-B', the volumes of ligand-binding cavities at each dimer-dimer interface have
276 been calculated for a large number of structures representing thermal distortions of the crystal
277 structure of the wild type ligand-free TTR tetramer (PDB 1F41). Volumes are obtained combining
278 convex hull algorithm [32] and Delaunay triangulations.

279 Ligand-cavities are analyzed either considering all residues per subunit lining the cavities,
280 listed on **Table 4**, or taking into account only the 10 residues that directly interact with a ligand as
281 defined in [33]. **Fig 4** depicts the resulted distribution of ligand-cavity volumes for each of the
282 cavities at the A-A' and B-B' interfaces. As can be seen, thermal fluctuations reveal differences in
283 size and flexibility for ligand cavities at each dimer-dimer interface. This is observed for both types
284 of cavities, defined either using all residues lining the cavities or only those residues interacting
285 with the ligand.

286

287 **Table 4. Residues that define TTR ligand-cavity.**

LEU 12	GLU 54	LEU 111
MET 13	LEU 55	SER 112
VAL 14	HIS 56	SER 115
LYS 15	GLY 57	TYR 116

VAL 16	ARG 104	SER 117
LEU 17	TYR 105	THR 118
ASP 18	THR 106	THR 119
SER 50	ILE 107	ALA 120
GLU 51	ALA 108	VAL 121
SER 52	ALA 109	VAL 122
GLY 53	LEU 110	THR 123

288 Residues at the Halogen Binding Pocket, as defined in ref [33], are denoted in red.

289

290 **Fig 4. Ligand-binding cavities and their corresponding thermal fluctuations:** ligand-cavities
 291 are defined according to (a) the 33 residues per subunit and (b) only the 10 buried residues, all listed
 292 on **Table 4**. The corresponding distributions of volumes, calculated for a large number of structures
 293 representing thermal distortions of the crystal structure of the wild type ligand-free TTR tetramer
 294 (PDB 1F41), are depicted for ligand-cavities either at the A-A' (black) or at B-B' (red) interfaces,
 295 respectively.

296

297 Here, normal mode analysis has been used to enlighten asymmetric aspects of TTR tetramer
 298 dynamics. While most of normal modes are delocalized between subunits A-A' and B-B' (**Fig 3**),
 299 several modes are mainly localized on one of them. In order to further analyze this finding, TTR-
 300 tetramer normal modes have been classified as follows. (1) *symmetric normal modes*: vibrations
 301 delocalized between subunits A-A' and B-B' with fractions of motions on subunit A-A' (**Fig 3**)
 302 within the range [0.45:0.55] and (2) *asymmetric modes*: modes localized preferentially on one
 303 subunit (fraction of motions on subunit A-A' <0.45 or > 0.55). Modes (2) can be further classified
 304 as (2a) *asymmetric modes by differences in relative amplitudes*: modes involving similar motions
 305 with different amplitudes on each subunit, (2b) *asymmetric modes by pairs*: modes displaying
 306 different motions on each subunit, but with a counterpart mode related to them by 2-fold rotational

307 symmetry, that is, involving equivalent motions but on the other subunit and (2c) *fully asymmetric*
308 *modes*: asymmetric modes that represent relative displacements on one subunit without a
309 counterpart on the other subunit. Following this classification, we have found that only 18.5%,
310 1.1% and 16.4% of modes correspond to types (1), (2a) and (2b) respectively, while 64% of modes
311 are fully asymmetric modes (2c).

312

313 **Discussion**

314 The molecular symmetry of multimeric proteins is generally determined by using X-ray
315 diffraction techniques, so that the basic question as to whether this symmetry is perfectly preserved
316 for proteins in solution remains open. In this respect, it should be pointed out that the crystal state
317 favors the presence of symmetrical objects, but, at the same time, different crystal contacts and
318 lattice constraints on different parts of the protein could alter its symmetry, introducing small, but
319 significant, deviations from the perfect symmetry. Despite the fact that crystal packing forces can
320 favor a particular sub-state of a protein, in general they are not believed to be strong enough to alter
321 significantly its tertiary and quaternary structures.

322 In the case of TTR, a tetrameric molecule characterized by three perpendicular two-fold
323 axes, one would expect in solution, where crystal contacts and constraints are absent, an ideal, fully
324 symmetrical tetramer. Subunits that are labeled A and B (and A' and B') in the crystal become
325 indistinguishable in solution. On the other hand, the presence of a strong binding heterogeneity for
326 the TTR tetramer in solution suggests that its functional properties are highly affected by
327 conformational changes, allowed by a protein structural flexibility that could not be revealed by X-
328 ray crystallography, a technique that can provide only static structural models trapped in a three-
329 dimensional lattice. Indeed, in a previous work, a molecular dynamics simulation has suggested that
330 in solution the TTR tetramer is quite flexible and that concerted movements affect the relative
331 orientation of subunits [7]. During these structural fluctuations, the two cavities of TTR become

332 larger and smaller in comparison with the theoretical size generated by a perfect 222 symmetry. It
333 was so postulated that the crystallization conditions may select one specific state of the tetramer,
334 perhaps more (or less) symmetrical as compared to that present in solution.

335 In this work, taking advantage of the crystallization of a TTR mutant form which
336 crystallizes with one single monomer in the asymmetric unit, we have examined and compared in
337 depth the aspects of the symmetry of the TTR tetramer in five different crystal forms, with the
338 presence of a different protein aggregation state in the asymmetric unit. This analysis shows that the
339 orientation of the four monomers relative to each other can change significantly, inducing in such a
340 way some changes in T4 binding cavities. Most importantly, when only one monomer is present in
341 the asymmetric unit and the tetramer is generated by the crystallographic two-fold axes, the perfect
342 symmetry of the tetramer is observed, whilst in the presence of a dimer or of a tetramer in the
343 asymmetric unit a significant deviation from the ideal 222 symmetry is observed.

344 The results of normal mode analysis are in full agreement with the previous conclusions:
345 they indicate that most of TTR-tetramer vibrations do not present 2-fold rotational symmetry
346 relative to the crystallographic axis that separates subunits A-A' and B-B'. Moreover, only a few of
347 them represent vibrations that are replicated on both subunits. Therefore, it is expected that these
348 asymmetries on vibrational patterns of subunits A-A' and B-B' should be reflected on different
349 dynamical properties relevant for ligand-binding. The asymmetric vibrational patterns for both
350 dimers lead to differential thermal structural distortions and consequent differential functional
351 properties for both ligand cavities.

352 It is well established that the two binding sites of TTR are characterized by two K_d values
353 for most ligands [5] [10] [34], with the second one often being more than one or two orders of
354 magnitude larger in comparison with the first one. A negative cooperativity effect for ligand
355 binding cannot simply be explained on the basis of the several crystal structures of TTR present in
356 the PDB, since in general the two binding sites are very similar and differences, when present, are
357 smaller than the standard deviation of the measurement. This also happens when one of the two

358 binding sites is empty or not fully occupied [7]. Our data strongly support the hypothesis that the
359 two binding cavities of TTR can be different, and that it is the crystallization process that selects a
360 specific conformational sub-state of the tetramer. Accordingly, the flexibility of the tetrameric
361 protein scaffold in solution would permit a dynamic reorientation of subunits, and a consequent
362 repositioning of residues lining the two binding cavities. As a consequence of previously discussed
363 asymmetries in the vibrational patterns of both subunits A-A' and B-B', thermal fluctuations leads
364 to differences in size and flexibility for ligand cavities at each dimer-dimer interface (see **Fig 4**).
365 These differences are larger between expanded cavities, defined by all residues at their surface, than
366 between smaller cavities, defined by only those residues interacting with the ligand. Therefore, our
367 results point out to potential differences on either ligand binding and ligand entrance. The binding
368 of a ligand to one of the two cavities, the most favorable one at the moment of binding, possibly
369 freezes the conformation of the tetramer in a slightly asymmetric state, leaving the other binding
370 site in a less favorable conformation for the binding of a second molecule. The second K_d is
371 generally larger than the first one, but the binding still takes place, suggesting that the perturbation
372 of the second binding site is relatively small. Owing to the flexibility of the TTR scaffold, the
373 crystallization process could force the tetramer towards a more symmetrical conformation as
374 compared to the state of the protein in solution. This may explain the finding of a rather
375 symmetrical arrangement of the subunits forming the T4 binding site in the TTR tetramer in the
376 crystal, at variance with their remarkable functional heterogeneity in solution.

377

378 **Conclusions**

379 It is worth wondering whether the behavior described in this paper is peculiar to TTR, or can
380 be of more general significance for multimeric proteins made by identical subunits and
381 characterized by some kind of rotational symmetry. Based on the crystal structure, it is generally
382 assumed that a perfect symmetry structurally characterizes these proteins in solution, so that a

383 functional symmetry is also inferred. Taking into account that the crystallization process favors the
384 presence of symmetrical molecules in the crystal, and on the basis of the results presented here, the
385 above conclusion could not be always justified.

386

387 **Acknowledgments**

388 We thank the staff of beamline ID30B of the European Synchrotron Radiation Facility (ESRF,
389 Grenoble, France) for technical assistance during data collection.

390

391 **Data Deposition**

392 Atomic coordinates and structure factors have been deposited at the Protein Data Bank (PDB) for
393 immediate release as 5OQ0

394

395 **References**

- 396 1. Wojtczak A, Cody V, Luft J, Pangborn W. Structures of human transthyretin complexed with
397 thyroxine at 2.0 Å resolution and 3', 5'-dinitro-N-acetyl-L-thyronine at 2.2 Å resolution.
398 *Acta Crystallogr D Biol Crystallogr*. 1996;52: 758–765.
- 399 2. Monaco HL, Rizzi M, Coda A. Structure of a complex of two plasma proteins: transthyretin
400 and retinol-binding protein. *Science*. 1995;268: 1039–1041.
- 401 3. Blake CC, Geisow MJ, Oatley SJ, Rérat B, Rérat C. Structure of prealbumin: secondary,
402 tertiary and quaternary interactions determined by Fourier refinement at 1.8 Å. *Journal of*
403 *Molecular Biology*. 1978;121: 339–356.
- 404 4. Hörnberg A, Eneqvist T, Olofsson A, Lundgren E, Sauer-Eriksson AE. A comparative
405 analysis of 23 structures of the amyloidogenic protein transthyretin. *Journal of Molecular*
406 *Biology*. 2000;302: 649–669. doi:10.1006/jmbi.2000.4078
- 407 5. Ferguson RN, Edelhofer H, Saroff HA, Robbins J, Cahnmann HJ. Negative cooperativity in
408 the binding of thyroxine to human serum prealbumin. Preparation of tritium-labeled 8-
409 anilino-1-naphthalenesulfonic acid. 1975;14: 282–289.
- 410 6. Florio P, Folli C, Cianci M, Del Rio D, Zanotti G, Berni R. Transthyretin Binding
411 Heterogeneity and Anti-amyloidogenic Activity of Natural Polyphenols and Their

- 412 Metabolites. *The Journal of biological chemistry*. American Society for Biochemistry and
413 Molecular Biology; 2015;290: 29769–29780. doi:10.1074/jbc.M115.690172
- 414 7. Cianci M, Folli C, Zonta F, Florio P, Berni R, Zanotti G. Structural evidence for asymmetric
415 ligand binding to transthyretin. *Acta Crystallogr D Biol Crystallogr*. 2015;71: 1582–1592.
416 doi:10.1107/S1399004715010585
- 417 8. Benson MD, Kincaid JC. The molecular biology and clinical features of amyloid neuropathy.
418 *Muscle Nerve*. 2007;36: 411–423. doi:10.1002/mus.20821
- 419 9. Connelly S, Choi S, Johnson SM, Kelly JW, Wilson IA. Structure-based design of kinetic
420 stabilizers that ameliorate the transthyretin amyloidoses. *Curr Opin Struct Biol*. 2010;20: 54–
421 62. doi:10.1016/j.sbi.2009.12.009
- 422 10. Bulawa CE, Connelly S, DeVit M, Wang L, Weigel C, Fleming JA, et al. Tafamidis, a potent
423 and selective transthyretin kinetic stabilizer that inhibits the amyloid cascade. *Proceedings of
424 the National Academy of Sciences of the United States of America*. 2012;109: 9629–9634.
425 doi:10.1073/pnas.1121005109
- 426 11. Zanotti G, Cendron L, Folli C, Florio P, Imbimbo BP, Berni R. Structural evidence for native
427 state stabilization of a conformationally labile amyloidogenic transthyretin variant by
428 fibrillogenesis inhibitors. *FEBS letters*. 2013;587: 2325–2331.
429 doi:10.1016/j.febslet.2013.06.016
- 430 12. Sant'Anna R, Gallego P, Robinson LZ, Pereira-Henriques A, Ferreira N, Pinheiro F, et al.
431 Repositioning tolcapone as a potent inhibitor of transthyretin amyloidogenesis and associated
432 cellular toxicity. *Nat Commun*. 2016;7: 10787. doi:10.1038/ncomms10787
- 433 13. Jiang X, Smith CS, Petrassi HM, Hammarström P, White JT, Sacchettini JC, et al. An
434 engineered transthyretin monomer that is nonamyloidogenic, unless it is partially denatured.
435 *Biochemistry*. 2001;40: 11442–11452. doi:10.1021/bi011194d
- 436 14. Pasquato N, Berni R, Folli C, Alfieri B, Cendron L, Zanotti G. Acidic pH-induced
437 conformational changes in amyloidogenic mutant transthyretin. *Journal of Molecular
438 Biology*. 2007;366: 711–719. doi:10.1016/j.jmb.2006.11.076
- 439 15. Kabsch W. XDS. *Acta Crystallogr D Biol Crystallogr*. 2010;66: 125–132.
440 doi:10.1107/S0907444909047337
- 441 16. Evans P. Scaling and assessment of data quality. *Acta Crystallogr D Biol Crystallogr*.
442 2006;62: 72–82. doi:10.1107/S0907444905036693
- 443 17. Winn MD, Ballard CC, Cowtan KD, Dodson EJ, Emsley P, Evans PR, et al. Overview of the
444 CCP4 suite and current developments. *Acta Crystallogr D Biol Crystallogr*. 2011;67: 235–
445 242. doi:10.1107/S0907444910045749
- 446 18. Adams PD, Afonine PV, Bunkóczi G, Chen VB, Davis IW, Echols N, et al. PHENIX: a
447 comprehensive Python-based system for macromolecular structure solution. *Acta Crystallogr
448 D Biol Crystallogr*. 2010;66: 213–221. doi:10.1107/S0907444909052925
- 449 19. Emsley P, Cowtan K. Coot: model-building tools for molecular graphics. *Acta Crystallogr D
450 Biol Crystallogr*. 2004;60: 2126–2132. doi:10.1107/S0907444904019158

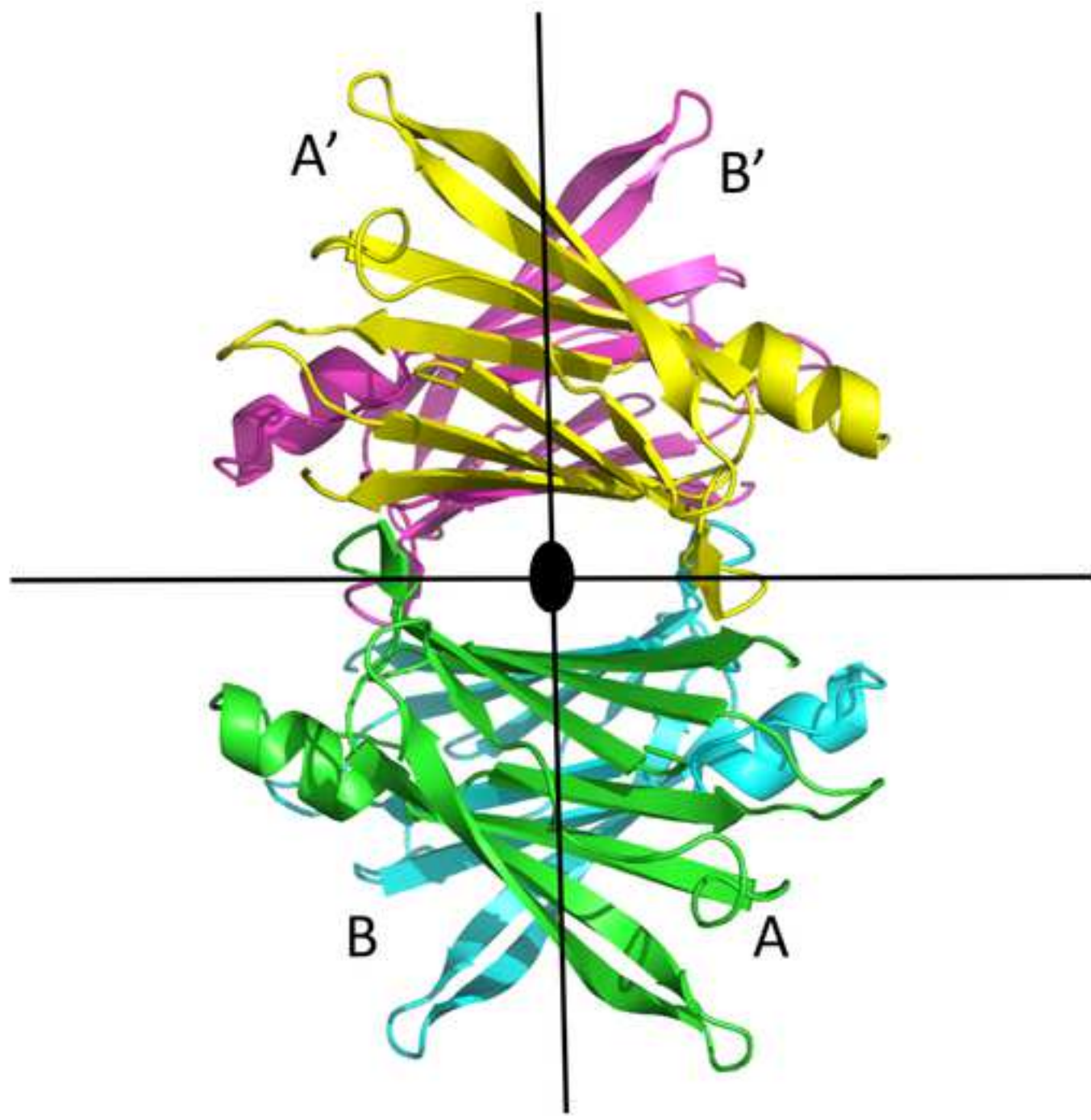
- 451 20. Tirion M. Large Amplitude Elastic Motions in Proteins from a Single-Parameter, Atomic
452 Analysis. *Phys Rev Lett*. American Physical Society; 1996;77: 1905–1908.
453 doi:10.1103/PhysRevLett.77.1905
- 454 21. Bahar I, Erman B, Jernigan RL, Atilgan AR, Covell DG. Collective motions in HIV-1
455 reverse transcriptase: Examination of flexibility and enzyme function. *Journal of Molecular*
456 *Biology*. 1999;285: 1023–1037. doi:10.1006/jmbi.1998.2371
- 457 22. Bahar I, Jernigan RL. Cooperative fluctuations and subunit communication in tryptophan
458 synthase. *Biochemistry*. 1999;38: 3478–3490. doi:10.1021/bi982697v
- 459 23. Bahar I, Rader AJ. Coarse-grained normal mode analysis in structural biology. *Curr Opin*
460 *Struct Biol*. 2005;15: 586–592. doi:10.1016/j.sbi.2005.08.007
- 461 24. Bahar I, Atilgan AR, Erman B. Direct evaluation of thermal fluctuations in proteins using a
462 single-parameter harmonic potential. *Fold Des*. 1997;2: 173–181. doi:10.1016/S1359-
463 0278(97)00024-2
- 464 25. Hinsen K. Analysis of domain motions by approximate normal mode calculations. *Proteins*.
465 1998;33: 417–429.
- 466 26. Atilgan AR, Durell SR, Jernigan RL, Demirel MC, Keskin O, Bahar I. Anisotropy of
467 fluctuation dynamics of proteins with an elastic network model. *Biophysical Journal*.
468 2001;80: 505–515. doi:10.1016/S0006-3495(01)76033-X
- 469 27. Jeong JI, Jang Y, Kim MK. A connection rule for alpha-carbon coarse-grained elastic
470 network models using chemical bond information. *J Mol Graph*. 2006;24: 296–306.
471 doi:10.1016/j.jmgm.2005.09.006
- 472 28. Saldano TE, Monzon AM, Parisi G, Fernandez-Alberti S. Evolutionary Conserved Positions
473 Define Protein Conformational Diversity. Keskin O, editor. *PLoS Comput Biol*. 2016;12:
474 e1004775. doi:10.1371/journal.pcbi.1004775
- 475 29. Polsinelli I, Nencetti S, Shepard W, Ciccone L, Orlandini E, Stura EA. A new crystal form of
476 human transthyretin obtained with a curcumin derived ligand. *Journal of Structural Biology*.
477 2016;194: 8–17. doi:10.1016/j.jsb.2016.01.007
- 478 30. Sebastião M, Saraiva M, Damas A. The crystal structure of amyloidogenic Leu55→ Pro
479 transthyretin variant reveals a possible pathway for transthyretin polymerization into amyloid
480 fibrils. 1998;273: 24715.
- 481 31. Wojtczak A, Neumann P, Cody V. Structure of a new polymorphic monoclinic form of
482 human transthyretin at 3 Å resolution reveals a mixed complex between unliganded and T4-
483 bound tetramers of TTR. *Acta Crystallogr D Biol Crystallogr*. 2001;57: 957–967.
- 484 32. Barber CB, Dobkin DP, Huhdanpaa H. The Quickhull algorithm for convex hulls. *Acm*
485 *Transactions on Mathematical Software*. 1996;22: 469–483. doi:10.1145/235815.235821
- 486 33. Tomar D, Khan T, Singh RR, Mishra S, Gupta S, Surolia A, et al. Crystallographic Study of
487 Novel Transthyretin Ligands Exhibiting Negative-Cooperativity between Two Thyroxine
488 Binding Sites. Khan RH, editor. *PLoS ONE*. Public Library of Science; 2012;7: e43522.
489 doi:10.1371/journal.pone.0043522

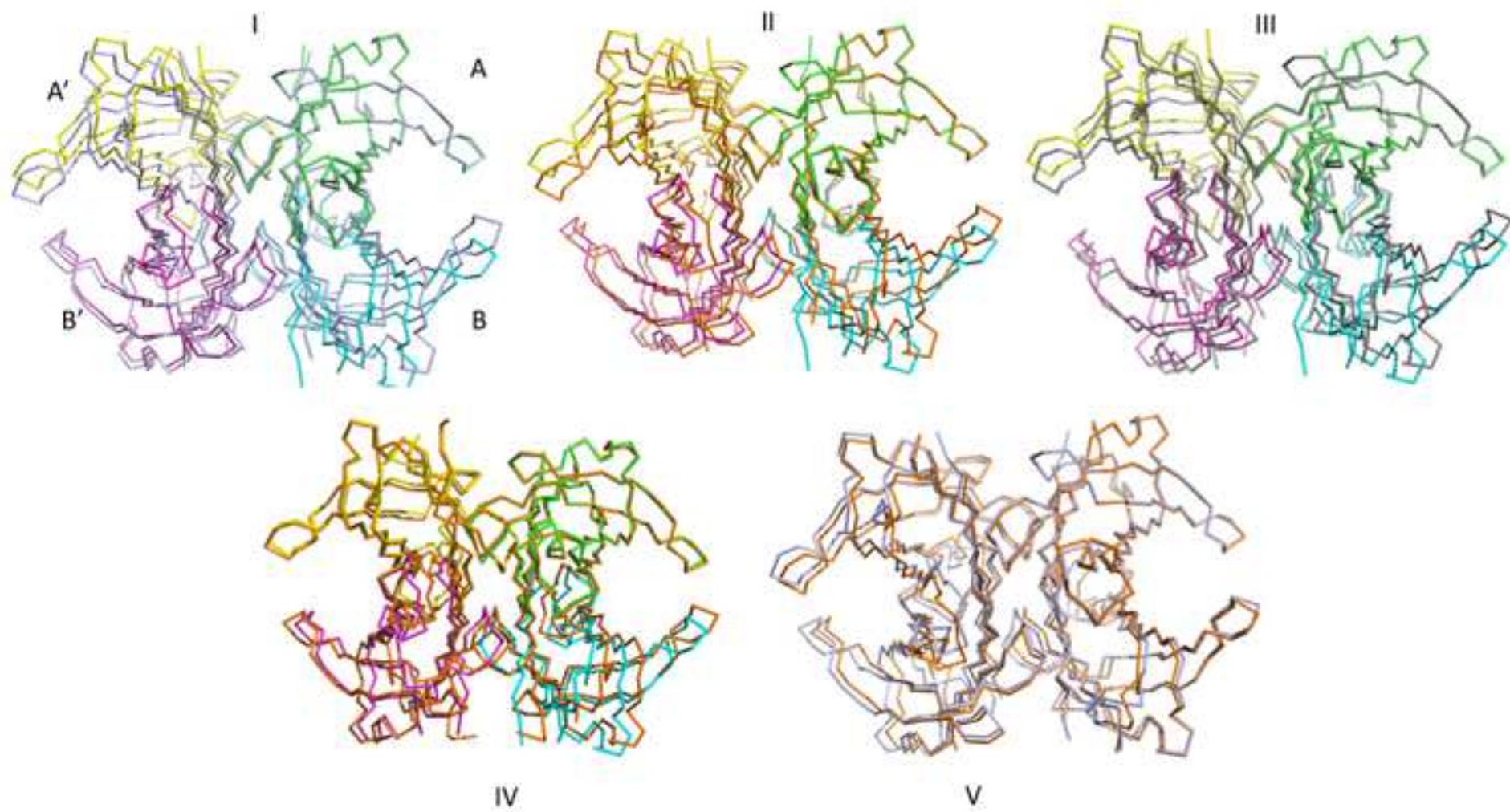
490 **34.** Johnson SM, Wiseman RL, Sekijima Y, Green NS, Adamski-Werner SL, Kelly JW. Native
491 state kinetic stabilization as a strategy to ameliorate protein misfolding diseases: a focus on
492 the transthyretin amyloidoses. *Acc Chem Res* 2005;38:911–921

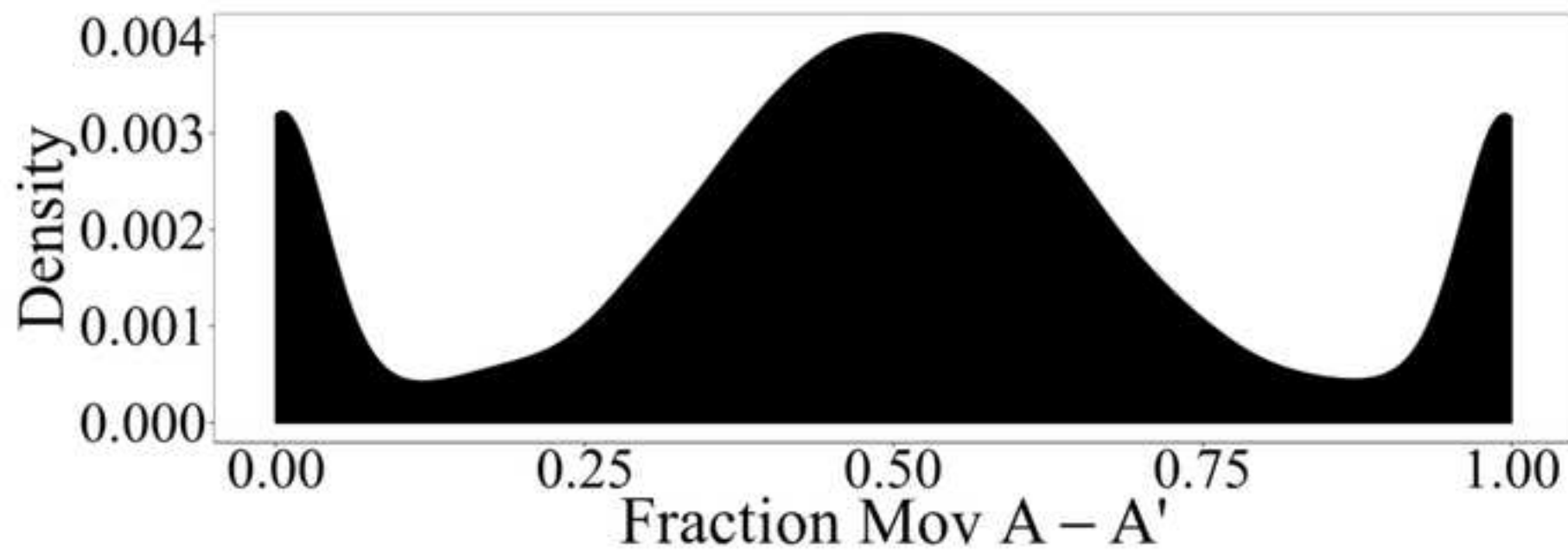
493 **35.** Davis IW, Leaver-Fay A, Chen VB, Block JN, Kapral GJ, Wang X, Murray LW, Arendall
494 WB III, Snoeyink J, Richardson JS and Richardson DC. MolProbity: all-atom contacts and
495 structure validation for proteins and nucleic acids. *Nucl. Acids Res.* 2007;35:W375-W383

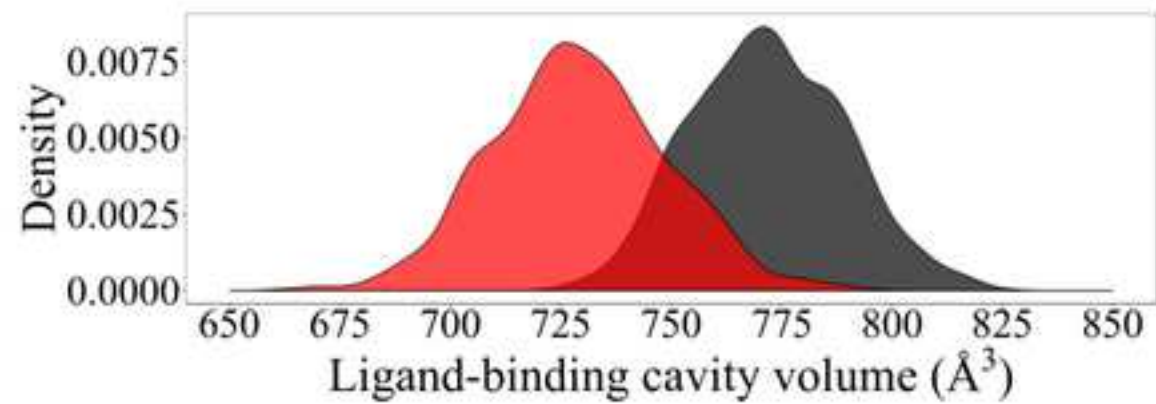
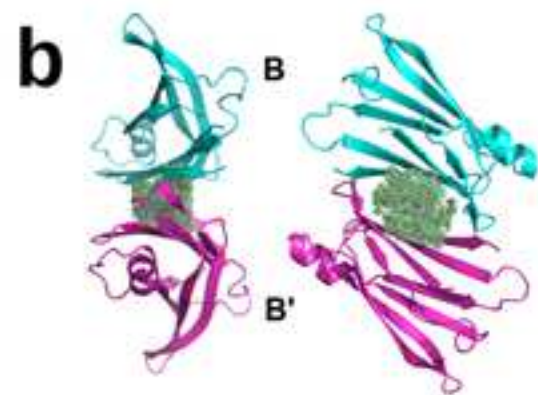
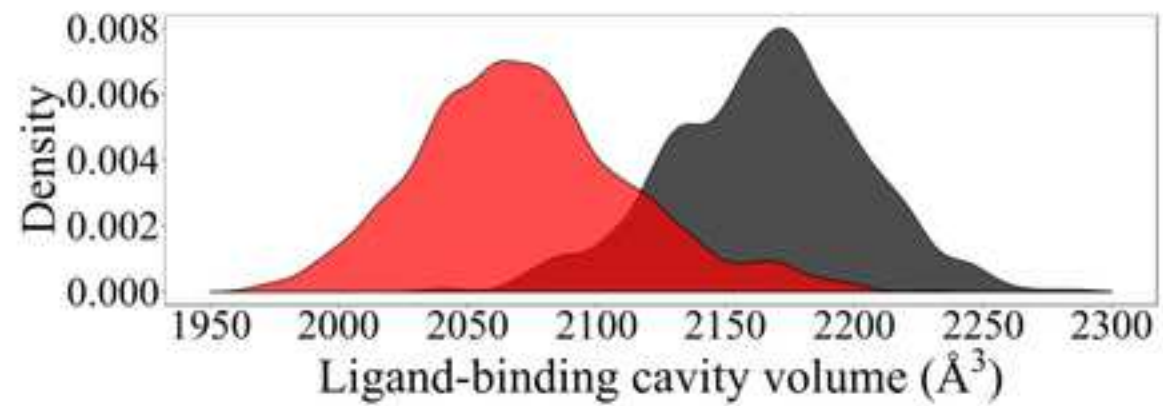
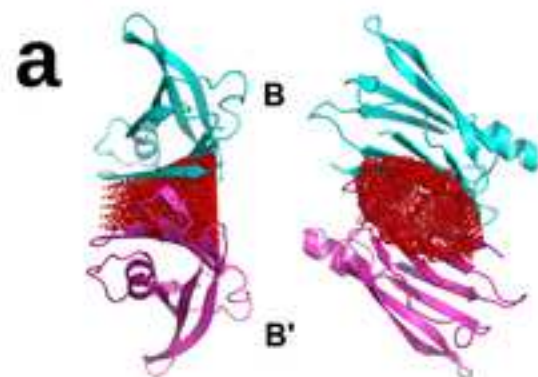
496

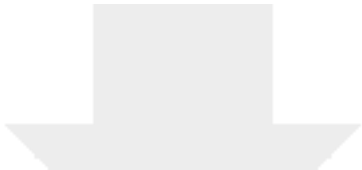
497 **Fig. S1. Aggregation states for mutant forms (F87M/L110M and F87M/L110M/S117E) of**
498 **human TTR in solution.** Wild type and mutant forms of human TTR, at a concentration of 0.5
499 mg/ml in 16 μ l of 50 mM sodium phosphate, 150 mM sodium chloride, pH 7.5, in the presence
500 (+T) or in the absence (-T) of 30 μ M tafamidis (dissolved in DMSO), were analyzed by SDS-PAGE
501 after quaternary structure fixation by incubation with 4 μ l of 25% (v/v) glutaraldehyde for 5
502 minutes at room temperature. The cross-linking reaction was terminated by the addition of 5 μ l of
503 sodium borohydrate (7% w/v in 0.1 M NaOH). Samples that were not cross-linked (NCL) were also
504 analyzed for a comparison.



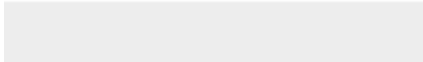









Click here to access/download
Supporting Information
S1_file.pdf





Click here to access/download
Other
validation_report_1.pdf



1
2
3
4
5
6
7
8
9
10
11
12
13
14
15
16
17
18

**STRUCTURAL AND DYNAMICS EVIDENCE FOR SCAFFOLD
ASYMMETRIC FLEXIBILITY OF THE HUMAN TRANSTHYRETIN
TETRAMER**

Giuseppe Zanotti ^{1*}, Francesca Vallese ¹, Alberto Ferrari ², Ilaria Menozzi ², Tadeo E. Saldaño³,
Paola Berto¹, Sebastian Fernandez-Alberti³, and Rodolfo Berni ²

¹ Department of Biomedical Sciences, University of Padua, Padua, Italy

² Department of Chemical Sciences, Life Sciences and Environmental Sustainability, University of
Parma, Parma, Italy

³ Universidad Nacional de Quilmes/CONICET, Bernal, Argentina

* Corresponding author

E-mail: giuseppe.zanotti@unipd.it

19 **Abstract**

20 The molecular symmetry of multimeric proteins is generally determined by using X-ray
21 diffraction techniques, so that the basic question as to whether this symmetry is perfectly preserved
22 for the same protein in solution remains open. In this work, human transthyretin (TTR), a
23 homotetrameric plasma transport protein with two binding sites for the thyroid hormone thyroxine
24 (T₄), is considered as a case study. **Based on the crystal structure of the TTR tetramer, a**
25 **hypothetical D₂ symmetry is inferred for the protein in solution, whose functional behavior reveals**
26 **the presence of two markedly different K_d values for the two T₄ binding sites. The latter property**
27 **has been ascribed to an as yet uncharacterized negative binding cooperativity.** A triple mutant form
28 of human TTR (F87M/L110M/S117E TTR), which is monomeric in solution, crystallizes as a
29 tetrameric protein and its structure has been determined. The exam of this and several other crystal
30 forms of human TTR suggests that the TTR scaffold possesses a significant structural flexibility. In
31 addition, TTR tetramer dynamics simulated using normal modes analysis exposes asymmetric
32 vibrational patterns on both dimers and thermal fluctuations reveal small differences in size and
33 flexibility for ligand cavities at each dimer-dimer interface. Such small structural differences
34 between monomers can lead to significant functional differences on the TTR tetramer dynamics, a
35 feature that may explain the functional heterogeneity of the T₄ binding sites, which is partially
36 overshadowed by the crystal state.

37

38 **Introduction**

39 Human transthyretin (TTR) is a homotetrameric protein involved in the transport in
40 extracellular fluids of thyroxine (T₄) and in the co-transport of vitamin A, by forming a
41 macromolecular complex with plasma retinol-binding protein [1,2]. Its structure was determined in
42 the late seventies and is now known at high resolution [3,4]. The TTR monomer is composed of two
43 four-stranded anti-parallel β -sheets and a short α -helix; two monomers are held together to form a

44 very stable dimer through a net of H-bond interactions involving the two edge β -strands H and F, in
45 such a way that a pseudo-continuous eight-stranded β -sandwich is generated, in which H and F β -
46 strands from each monomer in the dimer are connected to each other by main-chain H-bonds and
47 H-bonded water molecules. Structurally, the TTR tetramer is a dimer of dimers, in which the two
48 dimers associate, interacting mostly through hydrophobic contacts between residues of the AB and
49 GH loops. The assembly of the four identical subunits in TTR is highly symmetrical, being
50 characterized by 222 symmetry. A long channel, coincident with one of the 2-fold symmetry axes,
51 transverses the whole protein and harbors two T4 binding sites at the dimer-dimer interface.

52 Despite the presence in the TTR tetramer of two identical binding sites, which are both
53 occupied in the crystal with roughly similar mode of binding by T4 [1], its binding in solution is
54 characterized by a strong negative cooperativity, with about two order of magnitude difference in
55 the K_d values for the first and second T4 bound to TTR [5]. Recently, additional evidence for TTR
56 binding site heterogeneity both in solution, using the polyphenol resveratrol as a fluorescent ligand
57 [6], and in the crystal [7], has been obtained. More than 240 crystal structures of TTR in complex
58 with a variety of chemically different ligands, whose binding often exhibits negative cooperativity,
59 are present to date in the Protein Data Bank. Nevertheless, the molecular basis of the cooperative
60 behavior and of the heterogeneity of T4 binding sites remains to be clarified.

61 Human TTR and a number of its mutant forms have been associated with amyloid diseases
62 [8]. Amyloidoses are generated by the misfolding, misassembly and pathological aggregation of
63 several proteins, among which human TTR represents a remarkable example. Evidence has been
64 obtained by JW Kelly and coworkers to indicate that the rate-limiting dissociation of the native
65 tetrameric state into monomers, followed by misfolding of TTR monomers and their downhill
66 polymerization, leads to the formation of protein aggregates *in vitro*, and presumably *in vivo* ([9],
67 and references therein). Following these observations, the properties of a large number of TTR
68 ligands have been investigated in prospect of their use as drugs effective in the therapy of TTR

69 amyloidosis. In fact, T4 and other specific TTR ligands are able to stabilize the TTR tetramer and to
70 inhibit protein aggregation by occupying the T4 binding sites and establishing interactions that
71 connect the couple of subunits that form each binding site [9] [10] [11] [12]. Interestingly, it has
72 been inferred that the degree of negative binding cooperativity of a ligand is inversely related to its
73 ability to saturate and stabilize the TTR tetramer, so that features related to binding cooperativity
74 may also be relevant with regard to the anti-amyloidogenic potential of ligands [12].

75 Consistent with the observation that monomeric TTR may represent a key species along the
76 pathway of TTR amyloidogenesis, two mutations (F87M-L110M) able to induce the dissociation of
77 TTR into monomers were found to drastically accelerate protein aggregation *in vitro* [13]. An
78 additional mutation (S117E) has been introduced here in the sequence of the double TTR mutant, to
79 obtain a triple mutant, which is characterized by a stronger tendency to dissociate into the
80 monomeric state in solution, in comparison with the double mutant. However, crystal packing in the
81 presence of high protein concentration led to the formation of the TTR tetramer, whose structure
82 has been determined. Here, we report on the comparison of structural features of the triple
83 F87M/L110M/S117E TTR mutant and of other, previously characterized, forms of human TTR,
84 both wild type and mutant forms, crystallized in different space groups. Our data provide evidence
85 for a significant structural flexibility and asymmetric dynamics of the scaffold of the TTR tetramer,
86 a feature that leads to asymmetric functional properties of this protein in solution, such as those
87 associated with its putative cooperative behavior.

88 **Materials and methods**

89 **Crystallization and structure determination**

90 Recombinant mutant forms (F87M/L110M and F87M/L110M/S117E) of human TTR were
91 prepared by site-directed mutagenesis essentially as described [14]. Crystals of the triple
92 (F87M/L110M/S117E) TTR mutant were grown using the hanging-drop vapor diffusion method. 2

93 μ l of protein (7.3 mg/ml) solution in 50mM Tris-HCl (pH 8.0), 1 M ammonium sulfate, were
94 equilibrated against a well solution (100 μ l) containing 0.1 M sodium phosphate (pH 7.5), 2.2 M
95 ammonium sulfate. Single crystals of approximate size 0.02 mm in the longest dimension were
96 obtained in about a week of incubation at room temperature. 1500 images with an oscillation of
97 0.15° each were collected at the ID30B beamline of European Synchrotron Radiation Facility
98 (ESRF, Grenoble, France) for a total exposure time of 55.5 s. The crystal belongs to the space group
99 I222, with one monomer in the asymmetric unit. Datasets were processed with the software XDS
100 [15] and scaled with Scala [16] contained in the CCP4 suite [17]. The space group is I222, with one
101 monomer per asymmetric unit ($V_M = 2.05$, estimated solvent content 40%). The physiological
102 tetramer is generated through the crystallographic two-fold axes. The structure was solved by
103 molecular replacement using as a template one monomer of wild-type TTR in the P2₁2₁2 space
104 group (PDB ID 4W00, [7]) and refined using the package Phenix [18]. In the last cycles, TLS
105 refinement was applied. Map visualization and manual adjustment of the models were performed
106 using the Coot graphic interface [19]. Statistics on data collection and refinement are reported in
107 Table 1.

108 ~~pKa calculations~~

109 ~~The pKa values of ionizable residues were calculated by means of the program PROPKA,~~
110 ~~embedded in the software package PDB2PQR. The calculation was carried out at pH 7.0, using the~~
111 ~~F87M/L110M/S117E TTR mutant in monomeric and tetrameric states.~~

112

113 **Table 1. Data collection and refinement statistics.**

114

Data set	TTR I222
Wavelength (Å)	0.973186

Cell dimensions <i>a</i> , <i>b</i> , <i>c</i> (Å)	42.25 67.045 83.57
Resolution (Å)	52.29 - 1.94 (2.01 -1.94)*
Reflections (unique)	8849 (687)
<i>R</i> _{merge}	0.073 (0.916)
<i>R</i> _{pim}	0.030 (0.514)
$\langle I/\sigma(I) \rangle$	13.0 (1.6)
$\langle CC(1/2) \rangle$	0.998 (0.396)
Completeness (%)	97.4 (80.5)
Redundancy	7.2 (4.8)
Refinement	
No. reflections	8841
<i>R</i> _{work} / <i>R</i> _{free}	0.2296 (0.310) / 0.2671(0.347)
No. protein / solvent atoms	896 / 25
R.m.s. deviations	
Bond lengths (Å)	0.008
Bond angles (°)	0.944
Ramachandran plot	
Favored /outliers (%)	96.5 / 0.0
Rotamer outliers (%) / Cβ- outliers	2.1 / 0
Overall MolProbity score**	1.54

115

116 * Numbers in parentheses refer to the last resolution shell

117 ** See reference [35]

118 **Normal modes analysis**

119 Normal mode analysis has been calculated using the Elastic Network Model (ENM) [20] [21] [22]
120 [23] [24]. The model represents a protein structure as a network of N nodes. Herein, we have
121 considered as nodes the atoms of protein backbone, C_β and the center of mass of side chains.
122 Springs connect each node to their neighbors within a cut-off distance $r_c = 7\text{\AA}$. The resulted
123 potential energy is defined, according to [20] [25] [26], as

$$124 \quad E(\mathbf{r}_i, \mathbf{r}_j) = \frac{1}{2} k_{ij} (|\mathbf{r}_{ij}| - |\mathbf{r}_{ij}^0|)^2$$

125 where $\mathbf{r}_{ij} \equiv \mathbf{r}_i - \mathbf{r}_j$ is the vector connecting nodes i and j , and the zero superscript indicates the
126 position at the crystallographic structure. The value of the force constant k_{ij} varies according to the
127 type of interaction between nodes i and j [27] [28]. Normal modes are obtained as a set of
128 eigenvectors $\{\mathbf{Q}_i\}_{i=1, 3N}$ of the Hessian matrix, defined as the matrix of second-order partial
129 derivatives of the potential energy. Each \mathbf{Q}_i is a $3N$ vector whose elements $\{c_i^j\}_{j=1, 3N}$ represent the
130 relative displacements of Cartesian coordinates of each j^{th} residue. Therefore, for each normal mode
131 \mathbf{Q}_i , the fraction of relative displacements of residues belonging to subunit A-A' can be calculated
132 as $\sum_{j \in A-A'} (c_i^j)^2$.

133 **Set of structures representing thermal fluctuations**

134 A set of 1000 structures representing thermal distortions has been generated from the original X-ray
135 (PDB ID 1F41) uncomplexed TTR structure by randomly displacements in the direction of each
136 normal modes i within the range $[-A_i; A_i]$, being A_i (\AA) the corresponding amplitude of the mode at
137 room temperature

$$138 \quad A_i = \left(\frac{2k_B T}{\lambda_i} \right)^{1/2}$$

139 where k_B is the Boltzmann constant and T is the absolute temperature (300K). λ_i corresponds to the
140 eigenvalue associated to the i^{th} normal mode scaled in order to best fit the theoretical residue
141 fluctuations with the corresponding experimental temperature factors. The average root mean
142 square difference between structures was ~ 0.4 .

143

144 **Results**

145 **Crystal structure of the F87M/L110M/S117E TTR mutant form**

146 Out of a total of 240 human TTR structures present in the Protein Data Bank, 218 structures,
147 including those of several TTR mutant forms and TTR-ligand complexes, belong to the
148 orthorhombic space group $P2_12_12$. In such structures a dimer is present in the asymmetric unit, and
149 the second dimer is generated by symmetry, owing to the two-fold crystallographic axis coincident
150 with the central channel in the TTR tetramer. The resulting tetramer present in such crystal can
151 deviate from the ideal 222 symmetry, owing to the fact that only one of the two-fold axes is
152 coincident with the crystallographic one. On the contrary, crystals of the structure presented here
153 for the triple F87M/L110M/S117E TTR mutant belong to space group $I222$, where only one
154 monomer is present in the asymmetric unit, and the tetramer is generated by the crystallographic
155 symmetry (**Fig 1**). At variance with the structures obtained from crystals belonging to the space
156 group $P2_12_12$, in the centered $I222$ space group, the molecular symmetry of the protein is fully
157 coincident with the crystallographic one. The other known structure in this crystal form is that of
158 the V122I TTR mutant in complex with tolcapone [12]. In both cases the tetramer generated by the
159 crystallographic axes is equivalent to that of the already known structure of TTR [4].

160

161

162 **Fig 1. Cartoon view of the TTR tetramer.** The two black lines on the plane of the page and the
163 black dot in the center correspond to molecular two-fold axes. In the case of the $P2_12_12$ space
164 group, the central dot corresponds to the crystallographic two-fold axis, perpendicular to the plane
165 of the page. In the $I222$ space group, all **three** axes are crystallographic elements of symmetry.
166 **Chains are all identical, but they are labelled A and B or and A, B, C and D when a dimer or a**
167 **tetramer is present in the asymmetric unit, respectively.**

168

169 The final model in the I222 space group is essentially the same observed in the case of the
170 P2₁2₁2 crystal form. In fact, the r.m.s.d. for the superposition of 114 equivalent C α atoms of the
171 **monomer of the** triple F87M/L110M/S117E TTR mutant with those of a representative wt TTR
172 structure (PDB 1F41 [4] **is 0.52 Å for monomer A and 0.78 Å for monomer B**. Similar low r.m.s.d.
173 for the superposition of the wt TTR structure (PDB 1F41) to TTR crystallized in other space groups
174 are also found: 0.39 Å for the V122I TTR mutant in complex with tolcapone (PDB **5A6I** [12]);
175 0.45Å for the double F87M-L110M TTR mutant (PDB **1GKO** [13]); 0.60 Å for wt TTR in complex
176 with 4-hydroxy-chalcone (PDB 5EZP [29]); 0.74 Å for the monoclinic C2 crystals of the L55P TTR
177 mutant (PDB 5TTR [30]); 0.64 Å for the wt TTR monoclinic P2₁ crystals (PDB 1ICT [31]).

178 The triple F87M/L110M/S117E TTR mutant **in-solution** is characterized by a high
179 propensity to keep a monomeric state in solution, greater than that of the double F87M/L110M TTR
180 mutant, even in the presence of the strong fibrillogenesis inhibitor tafamidis [10] (**Fig S1**). The main
181 reason for the pronounced tetramer destabilization could be due to the presence of the side chains of
182 two pairs of Glu117, one towards the other, in the inner part of the cavity for each couple of
183 subunits (A-A' and B-B'). The distances between the two O ϵ 1 and O ϵ 2 of Glu117 residues of
184 subunits A and A' are in fact 5.15 Å and 5.06 Å, respectively, thereby generating a strong
185 electrostatic repulsion, provided that they are negatively charged. On the other hand, the distance
186 between two **O ϵ 2** atoms of Glu117 of subunits A and B' (and of B and A') is 2.79 Å in the crystal,
187 which is consistent with the formation of H bond interactions between each couple of the above
188 subunits **and, consequently, with the presence of tetrameric TTR in the crystal. The different**
189 **aggregation state found for the protein in the crystal and in solution may depend on contacts**
190 **between subunits and dimers induced by crystal lattice constraints and on differences in pKa values**
191 **of the carboxylic groups of Glu117 residues of the proteins in the two physical states.**

192

193

194 **Table 2. Calculated pKa for residue Glu 117.**

	pKa in the monomeric form	pKa in the tetrameric form
Glu117, chain A	4.78	13.43
Glu117, chain B	/	12.23
Glu117, chain A ²	/	7.69
Glu117, chain B ²	/	6.50

195

196

197 Relationships between monomers for different TTR crystal forms

198 To analyze the structural differences induced by the presence or absence of the
 199 crystallographic symmetry for structures determined from crystals belonging to different space
 200 groups, we have compared several TTR structures, as follows: the triple F87M/L110M/S117E TTR
 201 mutant; the wild type TTR form (PDB 1F41 [4]), as representative of a high-resolution structure of
 202 wild type TTR; the double F87M/L110M TTR mutant, which crystallizes in the P2₁2₁2₁ space
 203 group with a tetramer in the asymmetric unit (PDB 1GKO, [13]); the V122I TTR mutant in
 204 complex with tolcapone (PDB 5A6I, [12]), the only other TTR structure containing a single
 205 monomer in the asymmetric unit; the wild type TTR in complex with 4-hydroxy-chalcone (PDB
 206 5EZP, [29]), which crystallizes in the P3₁ space group, with two tetramers in the asymmetric unit.
 207 In the latter case, only one tetramer was considered in the comparison. Data for the structure of the
 208 L55P TTR mutant (PDB 5TTR, [30]), crystallized in space group C2 with one tetramer and two
 209 dimers in the asymmetric unit, are not reported in detail, but the general behavior is the same, as
 210 established for the other TTR crystal forms.

211

212

213 **Fig. 2 Comparison of the structures of TTR from different crystal forms.** Superposition of C α
 214 chain traces of (I) triple F87M/L110M/S117E TTR mutant to 1F41 structure, (II) triple TTR mutant
 215 to 56A1 structure, (III) triple TTR mutant to double TTR mutant **1GKO** structure, (IV) triple TTR
 216 mutant to 5EZP structure, (V) 1F41 to 56A1 structures. **In all cases, only monomers A were**
 217 **superimposed.** The four monomers of the TTR triple mutant are shown in different colors, the
 218 others in the same color.

219

220 If the C α atoms of one subunit, say A, are superimposed, we can visualize the differences in
 221 the position of the other subunits in relationships with that of subunit A for different crystal
 222 structures/space groups (**Fig 2**). In **Table 2**, a more quantitative estimate of the differences is given
 223 by the measure of the distances between equivalent C α atoms for subunits B, A' and B'. An
 224 analysis of these distances indicates that by superimposing monomers A of TTR tetramers from
 225 crystals belonging to different space groups, monomers B, A' and B' are displaced apparently in a
 226 random way. This indicates that taking monomer A as reference, the other monomers present a
 227 slightly different orientation for different crystal forms. For example, with the crystallographic two-
 228 fold axis of space group P2₁2₁2 running vertical in the page, by comparing the structures of the
 229 triple F87M/L110M/S117E TTR mutant and of wild type TTR (PDB 1F41), monomers B'
 230 superimpose quite well, whilst B and A' are significantly displaced (**Fig 2, panel I**). On the
 231 contrary, in the superposition of 1F41 and **5A6I** structures A and B are nearly coincident, while the
 232 positions of A' and B' diverge significantly (**Fig 2, panel IV**).

233

234 **Table 2. Interatomic distances between equivalent atoms in different TTR tetramers.**

	87/110/117	87/110/117	87/110/117	1F41 wild	87/110/117
	TTR mutant –	TTR mutant -	TTR mutant	typeTTR -	TTR mutant -
	wild type TTR	V122I TTR	- 87/110	V122I TTR	4-hydroxy-

	(1F41) *	mutant (5A6I)	TTR mutant (1GKO)	mutant (5A6I)	chalcone - TTR complex(5EZP)
Thr 96 B	2.44	1.71	2.02	0.98	2.37
Thr 96 C (A')	1.29	1.97	2.08	1.73	1.15
Thr 96 D (B')	2.38	1.42	2.58	2.69	2.36
Leu55 B	1.77	2.26	2.13	0.77	1.06
Leu55 C (A')	1.86	1.56	1.45	0.47	0.80
Leu55 D (B')	2.27	1.52	2.67	2.11	1.90
Ser85 B	3.52	0.96	0.99	3.03	2.37
Ser85 C (A')	3.42	2.39	3.27	2.65	2.26
Ser85 D (B')	3.98	2.83	2.48	1.81	2.68

235 Distances (in Å) between C α atoms for pair of proteins in subunits B, C and D, after superimposing
236 subunit A of the models. Residues of monomer A are not indicated, since they are practically
237 coincident.

238 *C and D labels correspond to A' and B' in the P2₁2₁2 space group, i.e. the crystallographic two-
239 fold axis superimposes A' to A and B' to B.

240

241 In turn, this situation has consequences on the size of TTR binding cavities. To give an
242 indication of the size of each of the two cavities, distances between corresponding C α atoms of
243 monomers A – A' and B – B' (i.e. the couples of subunits that line the two T4 binding cavities) are
244 compared in **Table 3**. Interestingly, these distances are in some cases quite different from one
245 structure to the other, a fact possibly due to real differences in the size of the cavity (also
246 considering that two of the reported structures are those of TTR mutant forms). However, such
247 differences could also partially reflect the slightly different cell parameters of the structures
248 considered. More relevant, since not affected by systematic errors, is the internal comparison

249 between the same distance between residues in the cavities formed by monomers A – A' and B – B'.

250 When only a TTR monomer is present in the asymmetric unit, i.e. a perfect tetramer is present in

251 the crystal, the two cavities are identical by symmetry; in the other cases, where a dimer or an entire

252 tetramer is present in the asymmetric unit, the two may differ in size. As expected, distances

253 between residues close to the center of the tetramer are less affected by the rotation of one monomer

254 relative to the other, whilst those far from the center of the tetramer present larger differences.

255 These differences are very small for wild type TTR (PDB 1F41), in which one dimer is present in

256 the crystal asymmetric unit, and definitely larger in cases where an entire tetramer is present in the

257 asymmetric unit, as for the 4-hydroxy-chalcone in complex with TTR and for the double

258 F87M/L110M TTR mutant. In the latter, the most astonishing difference is represented by residues

259 T119, for which there are more than 4Å differences in the distances between A – A' and B – B' (the

260 latter are labeled A – C and B – D in the original structure, since there is a tetramer in the

261 asymmetric unit). It must be considered anyhow that all the examined structures have been

262 determined at different resolutions.

263

264 **Table 3. Distances (in Å) between C α atoms of subunits A and C (or A') and B and D (or B').**

	87/110/117 TTR mutant	87/110 TTR mutant (1GKO)	V122I TTR mutant (5A6I)	wild type TTR (1F41)	4-hydroxy- chalcone - TTR complex (5EZP)
	A – A'	A – A' / B – B'	A – A'	A – A' / B – B'	A – A' / B – B'
S(E)117	9.67	9.54 / 9.92	8.75	9.36 / 9.30 (9.39)	9.83 / 9.86
T119	14.17	15.19 / 11.63	13.45	13.30 / 13.17	13.47 / 13.77

				(13.35)	
A108	11.70	10.45 / 11.82	11.98	11.84 / 11.86	11.56 / 11.73
K15	13.81	12.65 / 14.57	14.14	13.85 / 13.88	13.63 / 13.93
T106	17.72	17.82 / 16.27	17.59	17.94 / 17.80	17.84 / 18.30

265 In the case of the presence of a perfect tetramer in the asymmetric unit only one distance is
266 reported.

267

268 **Normal mode analysis of the TTR tetramer**

269 Using normal mode analysis, we have analyzed differences in the flexibilities of residues in the
270 couples of subunits A-A' and B-B', which form the two binding sites at the dimer-dimer interface
271 in the TTR tetramer. For this purpose, the fraction of relative displacements involving C α atoms of
272 subunit A-A' has been calculated for each normal mode of the wild type ligand-free TTR tetramer
273 (PDB 1F41). The distribution of these values is depicted in **Fig 3**. The peak at values of ~ 1
274 corresponds to normal modes entirely localized on the A-A' moiety, while normal modes localized
275 on the B-B' moiety are represented by the peak at ~ 0 . The maximum at ~ 0.5 indicates that most of
276 normal modes are equally distributed between both moieties. Nevertheless, the distribution is not
277 completely symmetric.

278

279

280 **Fig 3. Displacement of subunits.** Distribution of fraction of relative displacements involving C α
281 atoms of subunit A-A' evaluated on each normal mode of wild-type ligand-free TTR tetramer
282 normal modes.

283

284 In order to analyze functional aspects of the structural and dynamics asymmetries between
285 subunits A-A' and B-B', the volumes of ligand-binding cavities at each dimer-dimer interface have

286 been calculated for a large number of structures representing thermal distortions of the crystal
287 structure of the wild type ligand-free TTR tetramer (PDB 1F41). Volumes are obtained combining
288 convex hull algorithm [32] and Delaunay triangulations.

289 Ligand-cavities are analyzed either considering all residues per subunit lining the cavities,
290 listed on **Table 4**, or taking into account only the 10 residues that directly interact with a ligand as
291 defined in [33]. **Fig 4** depicts the resulted distribution of ligand-cavity volumes for each of the
292 cavities at the A-A' and B-B' interfaces. As can be seen, thermal fluctuations reveal differences in
293 size and flexibility for ligand cavities at each dimer-dimer interface. This is observed for both types
294 of cavities, defined either using all residues lining the cavities or only those residues interacting
295 with the ligand.

296

297 **Table 4. Residues that define TTR ligand-cavity.**

LEU 12	GLU 54	LEU 111
MET 13	LEU 55	SER 112
VAL 14	HIS 56	SER 115
LYS 15	GLY 57	TYR 116
VAL 16	ARG 104	SER 117
LEU 17	TYR 105	THR 118
ASP 18	THR 106	THR 119
SER 50	ILE 107	ALA 120
GLU 51	ALA 108	VAL 121
SER 52	ALA 109	VAL 122
GLY 53	LEU 110	THR 123

298 Residues at the Halogen Binding Pocket, as defined in ref [33], are denoted in red.

299

300 **Fig 4. Ligand-binding cavities and their corresponding thermal fluctuations:** ligand-cavities
301 are defined according to (a) the 33 residues per subunit and (b) only the 10 buried residues, all listed
302 on **Table 4**. The corresponding distributions of volumes, calculated for a large number of structures
303 representing thermal distortions of the crystal structure of the wild type ligand-free TTR tetramer
304 (PDB 1F41), are depicted for ligand-cavities either at the A-A' (black) or at B-B' (red) interfaces,
305 respectively.

306

307 Here, normal mode analysis has been used to enlighten asymmetric aspects of TTR tetramer
308 dynamics. While most of normal modes are delocalized between subunits A-A' and B-B' (see **Fig**
309 **3**), several modes are mainly localized on one of them. In order to further analyze this finding,
310 TTR-tetramer normal modes have been classified as follows. (1) *symmetric normal modes*:
311 vibrations delocalized between subunits A-A' and B-B' with fractions of motions on subunit A-A'
312 (**Fig 3**) within the range [0.45:0.55] and (2) *asymmetric modes*: modes localized preferentially on
313 one subunit (fraction of motions on subunit A-A' <0.45 or > 0.55). Modes (2) can be further
314 classified as (2a) *asymmetric modes by differences in relative amplitudes*: modes involving similar
315 motions with different amplitudes on each subunit, (2b) *asymmetric modes by pairs*: modes
316 displaying different motions on each subunit, but with a counterpart mode related to them by 2-fold
317 rotational symmetry, that is, involving equivalent motions but on the other subunit and (2c) *fully*
318 *asymmetric modes*: asymmetric modes that represent relative displacements on one subunit without
319 a counterpart on the other subunit. Following this classification, we have found that only 18.5%,
320 1.1% and 16.4% of modes correspond to types (1), (2a) and (2b) respectively, while 64% of modes
321 are fully asymmetric modes (2c).

322

323 **Discussion**

324

325 The molecular symmetry of multimeric proteins is generally determined by using X-ray
326 diffraction techniques, so that the basic question as to whether this symmetry is perfectly preserved
327 for proteins in solution remains open. In this respect, it should be pointed out that the crystal state
328 favors the presence of symmetrical objects, but, at the same time, different crystal contacts and
329 lattice constraints on different parts of the protein could alter its symmetry, introducing small, but
330 significant, deviations from the perfect symmetry. Despite the fact that crystal packing forces can
331 favor a particular sub-state of a protein, in general they are not believed to be strong enough to alter
332 significantly its tertiary and quaternary structures.

333 In the case of TTR, a tetrameric molecule characterized by three perpendicular two-fold
334 axes, one would expect in solution, where crystal contacts and constraints are absent, an ideal, fully
335 symmetrical tetramer. Subunits that are labeled A and B (and A' and B') in the crystal become
336 indistinguishable in solution. On the other hand, the presence of a strong binding heterogeneity for
337 the TTR tetramer in solution suggests that its functional properties are highly affected by
338 conformational changes, allowed by a protein structural flexibility that could not be revealed by X-
339 ray crystallography, a technique that can provide only static structural models trapped in a three-
340 dimensional lattice. Indeed, in a previous work, a molecular dynamics simulation has suggested that
341 in solution the TTR tetramer is quite flexible and that concerted movements affect the relative
342 orientation of subunits [7]. During these structural fluctuations, the two cavities of TTR become
343 larger and smaller in comparison with the theoretical size generated by a perfect 222 symmetry. It
344 was so postulated that the crystallization conditions may select one specific state of the tetramer,
345 perhaps more (or less) symmetrical as compared to that present in solution.

346 In this work, taking advantage of the crystallization of a TTR mutant form which
347 crystallizes with one single monomer in the asymmetric unit, we have examined and compared in
348 depth the aspects of the symmetry of the TTR tetramer in five different crystal forms, with the
349 presence of a different protein aggregation state in the asymmetric unit. This analysis shows that the
350 orientation of the four monomers relative to each other can change significantly, inducing in such a

351 way some changes in T4 binding cavities. Most importantly, when only one monomer is present in
352 the asymmetric unit and the tetramer is generated by the crystallographic two-fold axes, the perfect
353 symmetry of the tetramer is observed, whilst in the presence of a dimer or of a tetramer in the
354 asymmetric unit a significant deviation from the ideal 222 symmetry is observed.

355 The results of normal mode analysis are in full agreement with the previous conclusions:
356 they indicate that most of TTR-tetramer vibrations do not present 2-fold rotational symmetry
357 relative to the crystallographic axis that separates subunits A-A' and B-B'. Moreover, only a few of
358 them represent vibrations that are replicated on both subunits. Therefore, it is expected that these
359 asymmetries on vibrational patterns of subunits A-A' and B-B' should be reflected on different
360 dynamical properties relevant for ligand-binding. The asymmetric vibrational patterns for both
361 dimers lead to differential thermal structural distortions and consequent differential functional
362 properties for both ligand cavities.

363 It is well established that the two binding sites of TTR are characterized by two K_d values
364 for most ligands ([5], [10], [34]) with the second one often being more than one or two orders of
365 magnitude larger in comparison with the first one. A negative cooperativity effect for ligand
366 binding cannot simply be explained on the basis of the several crystal structures of TTR present in
367 the PDB, since in general the two binding sites are very similar and differences, when present, are
368 smaller than the standard deviation of the measurement. This also happens when one of the two
369 binding sites is empty or not fully occupied [7]. Our data strongly support the hypothesis that the
370 two binding cavities of TTR can be different, and that it is the crystallization process that selects a
371 specific conformational sub-state of the tetramer. Accordingly, the flexibility of the tetrameric
372 protein scaffold in solution would permit a dynamic reorientation of subunits, and a consequent
373 repositioning of residues lining the two binding cavities. As a consequence of previously discussed
374 asymmetries in the vibrational patterns of both subunits A-A' and B-B', thermal fluctuations leads
375 to differences in size and flexibility for ligand cavities at each dimer-dimer interface (see **Fig 4**).
376 These differences are larger between expanded cavities, defined by all residues at their surface, than

377 between smaller cavities, defined by only those residues interacting with the ligand. Therefore, our
378 results point out to potential differences on either ligand binding and ligand entrance. The binding
379 of a ligand to one of the two cavities, the most favorable one at the moment of binding, possibly
380 freezes the conformation of the tetramer in a slightly asymmetric state, leaving the other binding
381 site in a less favorable conformation for the binding of a second molecule. The second K_d is
382 generally larger than the first one, but the binding still takes place, suggesting that the perturbation
383 of the second binding site is relatively small. Owing to the flexibility of the TTR scaffold, the
384 crystallization process could force the tetramer towards a more symmetrical conformation as
385 compared to the state of the protein in solution. This may explain the finding of a rather
386 symmetrical arrangement of the subunits forming the T4 binding site in the TTR tetramer in the
387 crystal, at variance with their remarkable functional heterogeneity in solution.

388

389 **Conclusions**

390 It is worth wondering whether the behavior described in this paper is peculiar to TTR, or can
391 be of more general significance for multimeric proteins made by identical subunits and
392 characterized by some kind of rotational symmetry. Based on the crystal structure, it is generally
393 assumed that a perfect symmetry structurally characterizes these proteins in solution, so that a
394 functional symmetry is also inferred. Taking into account that the crystallization process favors the
395 presence of symmetrical molecules in the crystal, and on the basis of the results presented here, the
396 above conclusion could not be always justified.

397

398 **Acknowledgments**

399 We thank the staff of beamline ID30B of the European Synchrotron Radiation Facility (ESRF,
400 Grenoble, France) for technical assistance during data collection.

401 **Data Deposition**

402 **Atomic coordinates and structure factors have been deposited at the Protein Data Bank**
403 **(PDB) for immediate release as 5OQ0**

404

405 **Financial disclosure**

406 **This work received financial support from: Universities of Padua, www.unipd.it (GZ), and Parma,**
407 **www.unipr.it (RB), Italy; MIUR (Ministero Istruzione Universita` Ricerca, Rome, Italy) PRIN**
408 **(Progetti di Rilevante Interesse Nazionale, www.prin.miur.it) Project # 2012A7LMS3_002 (RB).**

409

410 **References**

- 411 1. Wojtczak A, Cody V, Luft J, Pangborn W. Structures of human transthyretin complexed with
412 thyroxine at 2.0 Å resolution and 3',5'-dinitro-N-acetyl-L-thyronine at 2.2 Å resolution.
413 *Acta Crystallogr D Biol Crystallogr.* 1996;52: 758–765.
- 414 2. Monaco HL, Rizzi M, Coda A. Structure of a complex of two plasma proteins: transthyretin
415 and retinol-binding protein. *Science.* 1995;268: 1039–1041.
- 416 3. Blake CC, Geisow MJ, Oatley SJ, Rérat B, Rérat C. Structure of prealbumin: secondary,
417 tertiary and quaternary interactions determined by Fourier refinement at 1.8 Å. *Journal of*
418 *Molecular Biology.* 1978;121: 339–356.
- 419 4. Hörnberg A, Eneqvist T, Olofsson A, Lundgren E, Sauer-Eriksson AE. A comparative
420 analysis of 23 structures of the amyloidogenic protein transthyretin. *Journal of Molecular*
421 *Biology.* 2000;302: 649–669. doi:10.1006/jmbi.2000.4078
- 422 5. Ferguson RN, Edelhofer H, Saroff HA, Robbins J, Cahnmann HJ. Negative cooperativity in
423 the binding of thyroxine to human serum prealbumin. Preparation of tritium-labeled 8-
424 anilino-1-naphthalenesulfonic acid. 1975;14: 282–289.
- 425 6. Florio P, Folli C, Cianci M, Del Rio D, Zanotti G, Berni R. Transthyretin Binding
426 Heterogeneity and Anti-amyloidogenic Activity of Natural Polyphenols and Their
427 Metabolites. *The Journal of biological chemistry.* American Society for Biochemistry and
428 *Molecular Biology;* 2015;290: 29769–29780. doi:10.1074/jbc.M115.690172
- 429 7. Cianci M, Folli C, Zonta F, Florio P, Berni R, Zanotti G. Structural evidence for asymmetric
430 ligand binding to transthyretin. *Acta Crystallogr D Biol Crystallogr.* 2015;71: 1582–1592.
431 doi:10.1107/S1399004715010585

- 432 8. Benson MD, Kincaid JC. The molecular biology and clinical features of amyloid neuropathy.
433 *Muscle Nerve*. 2007;36: 411–423. doi:10.1002/mus.20821
- 434 9. Connelly S, Choi S, Johnson SM, Kelly JW, Wilson IA. Structure-based design of kinetic
435 stabilizers that ameliorate the transthyretin amyloidoses. *Curr Opin Struct Biol*. 2010;20: 54–
436 62. doi:10.1016/j.sbi.2009.12.009
- 437 10. Bulawa CE, Connelly S, DeVit M, Wang L, Weigel C, Fleming JA, et al. Tafamidis, a potent
438 and selective transthyretin kinetic stabilizer that inhibits the amyloid cascade. *Proceedings of*
439 *the National Academy of Sciences of the United States of America*. 2012;109: 9629–9634.
440 doi:10.1073/pnas.1121005109
- 441 11. Zanotti G, Cendron L, Folli C, Florio P, Imbimbo BP, Berni R. Structural evidence for native
442 state stabilization of a conformationally labile amyloidogenic transthyretin variant by
443 fibrillogenesis inhibitors. *FEBS letters*. 2013;587: 2325–2331.
444 doi:10.1016/j.febslet.2013.06.016
- 445 12. Sant'Anna R, Gallego P, Robinson LZ, Pereira-Henriques A, Ferreira N, Pinheiro F, et al.
446 Repositioning tolcapone as a potent inhibitor of transthyretin amyloidogenesis and associated
447 cellular toxicity. *Nat Commun*. 2016;7: 10787. doi:10.1038/ncomms10787
- 448 13. Jiang X, Smith CS, Petrassi HM, Hammarström P, White JT, Sacchettini JC, et al. An
449 engineered transthyretin monomer that is nonamyloidogenic, unless it is partially denatured.
450 *Biochemistry*. 2001;40: 11442–11452. doi:10.1021/bi011194d
- 451 14. Pasquato N, Berni R, Folli C, Alfieri B, Cendron L, Zanotti G. Acidic pH-induced
452 conformational changes in amyloidogenic mutant transthyretin. *Journal of Molecular*
453 *Biology*. 2007;366: 711–719. doi:10.1016/j.jmb.2006.11.076
- 454 15. Kabsch W. XDS. *Acta Crystallogr D Biol Crystallogr*. 2010;66: 125–132.
455 doi:10.1107/S0907444909047337
- 456 16. Evans P. Scaling and assessment of data quality. *Acta Crystallogr D Biol Crystallogr*.
457 2006;62: 72–82. doi:10.1107/S0907444905036693
- 458 17. Winn MD, Ballard CC, Cowtan KD, Dodson EJ, Emsley P, Evans PR, et al. Overview of the
459 CCP4 suite and current developments. *Acta Crystallogr D Biol Crystallogr*. 2011;67: 235–
460 242. doi:10.1107/S0907444910045749
- 461 18. Adams PD, Afonine PV, Bunkóczi G, Chen VB, Davis IW, Echols N, et al. PHENIX: a
462 comprehensive Python-based system for macromolecular structure solution. *Acta Crystallogr*
463 *D Biol Crystallogr*. 2010;66: 213–221. doi:10.1107/S0907444909052925
- 464 19. Emsley P, Cowtan K. Coot: model-building tools for molecular graphics. *Acta Crystallogr D*
465 *Biol Crystallogr*. 2004;60: 2126–2132. doi:10.1107/S0907444904019158
- 466 20. Tirion M. Large Amplitude Elastic Motions in Proteins from a Single-Parameter, Atomic
467 Analysis. *Phys Rev Lett*. American Physical Society; 1996;77: 1905–1908.
468 doi:10.1103/PhysRevLett.77.1905
- 469 21. Bahar I, Erman B, Jernigan RL, Atilgan AR, Covell DG. Collective motions in HIV-1
470 reverse transcriptase: Examination of flexibility and enzyme function. *Journal of Molecular*
471 *Biology*. 1999;285: 1023–1037. doi:10.1006/jmbi.1998.2371

- 472 22. Bahar I, Jernigan RL. Cooperative fluctuations and subunit communication in tryptophan
473 synthase. *Biochemistry*. 1999;38: 3478–3490. doi:10.1021/bi982697v
- 474 23. Bahar I, Rader AJ. Coarse-grained normal mode analysis in structural biology. *Curr Opin*
475 *Struct Biol*. 2005;15: 586–592. doi:10.1016/j.sbi.2005.08.007
- 476 24. Bahar I, Atilgan AR, Erman B. Direct evaluation of thermal fluctuations in proteins using a
477 single-parameter harmonic potential. *Fold Des*. 1997;2: 173–181. doi:10.1016/S1359-
478 0278(97)00024-2
- 479 25. Hinsen K. Analysis of domain motions by approximate normal mode calculations. *Proteins*.
480 1998;33: 417–429.
- 481 26. Atilgan AR, Durell SR, Jernigan RL, Demirel MC, Keskin O, Bahar I. Anisotropy of
482 fluctuation dynamics of proteins with an elastic network model. *Biophysical Journal*.
483 2001;80: 505–515. doi:10.1016/S0006-3495(01)76033-X
- 484 27. Jeong JI, Jang Y, Kim MK. A connection rule for alpha-carbon coarse-grained elastic
485 network models using chemical bond information. *J Mol Graph*. 2006;24: 296–306.
486 doi:10.1016/j.jmgm.2005.09.006
- 487 28. Saldano TE, Monzon AM, Parisi G, Fernandez-Alberti S. Evolutionary Conserved Positions
488 Define Protein Conformational Diversity. Keskin O, editor. *PLoS Comput Biol*. 2016;12:
489 e1004775. doi:10.1371/journal.pcbi.1004775
- 490 29. Polsinelli I, Nencetti S, Shepard W, Ciccone L, Orlandini E, Stura EA. A new crystal form of
491 human transthyretin obtained with a curcumin derived ligand. *Journal of Structural Biology*.
492 2016;194: 8–17. doi:10.1016/j.jsb.2016.01.007
- 493 30. Sebastião M, Saraiva M, Damas A. The crystal structure of amyloidogenic Leu55→ Pro
494 transthyretin variant reveals a possible pathway for transthyretin polymerization into amyloid
495 fibrils. 1998;273: 24715.
- 496 31. Wojtczak A, Neumann P, Cody V. Structure of a new polymorphic monoclinic form of
497 human transthyretin at 3 Å resolution reveals a mixed complex between unliganded and T4-
498 bound tetramers of TTR. *Acta Crystallogr D Biol Crystallogr*. 2001;57: 957–967.
- 499 32. Barber CB, Dobkin DP, Huhdanpaa H. The Quickhull algorithm for convex hulls. *Acm*
500 *Transactions on Mathematical Software*. 1996;22: 469–483. doi:10.1145/235815.235821
- 501 33. Tomar D, Khan T, Singh RR, Mishra S, Gupta S, Surolia A, et al. Crystallographic Study of
502 Novel Transthyretin Ligands Exhibiting Negative-Cooperativity between Two Thyroxine
503 Binding Sites. Khan RH, editor. *PLoS ONE*. Public Library of Science; 2012;7: e43522.
504 doi:10.1371/journal.pone.0043522
- 505 **34.** Johnson SM, Wiseman RL, Sekijima Y, Green NS, Adamski-Werner SL, Kelly JW. Native
506 state kinetic stabilization as a strategy to ameliorate protein misfolding diseases: a focus on
507 the transthyretin amyloidoses. *Acc Chem Res* 2005;38:911–921
- 508 **35.** Davis IW, Leaver-Fay A, Chen VB, Block JN, Kapral GJ, Wang X, Murray LW, Arendall
509 WB III, Snoeyink J, Richardson JS and Richardson DC. MolProbity: all-atom contacts and
510 structure validation for proteins and nucleic acids. *Nucl. Acids Res*. 2007;35:W375-W383

511

512 **Fig. S1. Aggregation states for mutant forms (F87M/L110M and F87M/L110M/S117E) of**
513 **human TTR in solution.** Wild type and mutant forms of human TTR, at a concentration of 0.5
514 mg/ml in 16 μ l of 50 mM sodium phosphate, 150 mM sodium chloride, pH 7.5, in the presence
515 (+T) or in the absence (-T) of 30 μ M tafamidis (dissolved in DMSO), were analyzed by SDS-PAGE
516 after quaternary structure fixation by incubation with 4 μ l of 25% (v/v) glutaraldehyde for 5
517 minutes at room temperature. The cross-linking reaction was terminated by the addition of 5 μ l of
518 sodium borohydrate (7% w/v in 0.1 M NaOH). Samples that were not cross-linked (NCL) were also
519 analyzed for a comparison.

Reviewer #1: My comments below:

i) Authors state that "D2 symmetry is inferred for the protein in solution" (and I would ask if SAXS envelopes for protein alike have ever been obtained, or maybe data from DLS), "despite the fact that its two T4 binding sites are characterized by two markedly different K_d values". Why the use of "despite" here? Is this (different K_d) not expected in a "cooperativity" effect (which may arise even in a perfectly symmetrical protein, when this symmetry is "broken" once one site is filled)? Might they state better their point? It seems that the authors state the different K_d is independent of one site previously filled (therefore, two independent sites). AFAIU this is not the point in the article.

As suggested by the referee, this point has been better stated: Abstract, lines 25-28

ii) In M & M (lines 93/94), state volumes of each solution used to prepare the crystallization drop. Crystal dimensions would also be recommendable.

We have provided the experimental details requested by the referee: Materials and Methods, lines 94-96.

iii) Table 1: number of reflections overall, unique, observed? Though obvious, state unit also for wavelength. I would also claim for stating CC(1/2) values from data reduction.

These values have been added in the Table

iv) Any special comment for the relatively low rmsd values for bond lengths and bond angles?

The small r.m.s.d. is the result of the Phenix refinement and of the weighting scheme used. Lower restraints should probably be ended up with a lower R factor, but we have preferred to be conservative and to obtain a crystal structure with very good geometry.

v) Is the structure so densely packed, only 25 ordered solvent atoms? The protein is small, OK, but what is the estimated %(V/V) disordered solvent content?

The estimated solvent content is 40%. The number of solvent molecule is not so low, considering that resolution is 1.94Å and the solvent corresponds to one monomer. There are 100 solvent molecules per tetramer, this looks reasonable at this resolution.

vi) Overall score: what is that from? In table 1.

The overall MolProbity score defines the overall geometry quality of the structure. This number should be similar to resolution, if it is smaller it indicates that the geometry is better than the mean structures at the same resolution

vii) Line 148: it would be nice to have some indices (rmsd between Ca's?) to assert how much this deviation is.

R.m.s.d. in this context are not very significant, because they may reflect the differences of few loops. I think that distances between selected C α pairs reported in Table 3 (now Table 2) better reflect the deviation from the ideal 222 symmetry.

viii) Line 156: One concludes that all residues could be modeled in the electron density, no disorder for side chains or main chains, it would be nice to have this affirmed.

The monomer of TTR visible in the crystal is similar that the other structures

ix) Line 163, should be 'all axes' or maybe 'all three axes'...?

The text has been corrected

x) Line 168: just assert that the cited rmsd is for a tetramer superposition (the most obvious), such

that relative differences between positions of monomers of the same structure were not changed. It would be nice to know of this value when one superposes monomer by monomer.

No, all values are for the superposition of the monomer (since we have a monomer in the asymmetric unit). We have added r.m.s.d. for monomers A and B in the case of 1F41. Of course, we could have superimposed our monomer with all two or four monomers of each of the other structures, but numbers deviate slightly from one to the other and they are not really significant.

xi) Nice to see the picture S1, but one could consider, should that be easily available, either SAXS or DLS measurements to reinforce the observations. This might be bound to the fact that you find that in one pair of E117 one of them might be protonated, as mentioned through lines 190-193

We consider the evidence of Fig. S1 sufficient, also taking into account that the monomeric state of TTR is not the focus of the paper

xii) Line 179: I do not have access to the structure, but should not this lead to the dissociation into dimers, rather than monomers? Do you foresee repulsions also between subunits A and B?

With regard to the latter points, the text has been modified according to the suggestions of referee # 2, removing Table 2 and trying to summarize the hypotheses concerning the differences observed for the aggregation state of the triple mutant form of TTR in the crystal and in solution.

With regard to the use of techniques suited to better characterize structurally our triple mutant form of TTR, a species that might provide insight into the pathway of formation of amyloid fibrils, studies are currently being planned in our laboratory.

xiii) Line 182, I suppose these " O " are side chain Oxygens as well... Are they main chain oxygens? Please, inform.

Atom labels have been corrected.

xiv) Line 246: these comparisons might be enriched if the cavity volumes are also estimated. Of course, one has to care of disordered side chains that might absent in the structures.

An exact estimation of the cavity volume is hampered by the fact that the opening of the cavity is quite large and it is hard to define the limits of the cavity. In addition, flexible side chains of the residues around the cavity opening make it difficult to compare the values.

xv) Line 293: should it not be A A' for figure 4.a? Figure 4.b already shows B B'.

Figure 4.a and Figure 4.b (only the distribution) actually correspond to both ligand-cavities either at the A-A' (black) or at B-B' (red) interfaces. Figure 4.a considers volume cavities defined using the 33 residues lining each cavity, and Figure 4.b. considers volume cavities defined by the 10 residues that form the Halogen Binding Pocket.

In Figure 4.a. the structure corresponds to chains B-B'. It shows the volume cavities defined using the 33 residues lining each cavity, presented in Table 5. In Figure 4.b., again, the structure corresponds to chains B-B', but this image shows the volume cavities defined using the 10 residues that form the Halogen Binding Pocket. (and THR 118 and VAL 121), denote in red in Table 5.

The cavities formed by A-A' subunits are not shown as a Figure, only as a distribution.

xvi) Reference #35 is evoked, but the list finishes at #33.

A missing reference has been added and all have been renumbered, owing to the fact that two of them were neglected in the automatic conversion of the references.

Some typos?:

Line 98: "one monomers"

Thanks, corrected

Line 99: "243" ?

I apologize, the two references have been corrected

Line 112: though obvious, indicate units for wavelength

Done

Line 142: "truncated"

Line 193: "destabilizing", change for " destabilize"

This part has been omitted in the final version

Line 366: "order*s*"

Done

Reviewer #2: Human Transthyretin is a tetrameric human plasma protein that can misfold and cause amyloid disease. The protein's normal function is to bind thyroxine (T4) for which it has two binding pockets positioned at the 2-fold axis at the dimer-dimer interface.

Previous published data (including papers from the submitted authors) suggest that binding of ligands to the dimer-dimer interface is asymmetric, and includes negative cooperativity. In this paper Zanotti et al have used normal modes analysis to study TTR tetramer dynamics. A new crystal structure of a triple mutant is also presented, however, I find this structure to be of limited value for the conclusions drawn.

Originally, we decided to crystallize the triple mutant since we expected to obtain crystals of the monomer, since the mutated protein is mostly monomeric in solution. On the contrary, the crystallization process selects the tetrameric form. Nevertheless, we used this structure to compare representative crystal structures of TTR in three different situations, i.e. when a monomer, a dimer and a tetramer is present in the asymmetric unit, in the hope to observe differences among inter-subunit distances not influenced by crystal packing. Our hypothesis, confirmed by normal mode analysis, is that the tetramer is quite flexible in solution (and that this flexibility is mostly due to relative movements of the entire monomers), whilst the crystallization process "freezes" the tetramer in a symmetric quaternary structure.

I find that the paper contains results from a mixture of studies that is not clearly inter-connected. For example what is the point with the performed pKa calculations? Also the calculated pKa value of 13 for a Glu seems too unrealistic. Remove Table 2 from the paper is my advice. The data presented in Table 3 and 4 does also not feel new. Many, including the authors themselves, have noticed and published measured differences in the size of the binding cavities. The authors could also do a better job helping the reader to understand the data presented. For example in Figure 4, what is hiding under the word "density" on the Y-axis?

See also comments above. Table 2 and data on pKa have been removed.

About Table 3 and 4, we agree that differences have been published in various papers. Nevertheless, differences in the two cavities are very small and generally observed in structures whose resolution is not high. In this paper we have done a systematic comparison and our analysis suggests that differences observed in the two cavities are not really indicative of a difference among structures, but more likely of fluctuations around a perfectly symmetric tetramer.

Minor issues:

The manuscript contains many "minor" but frustrating mistakes

1) references: are given both in brackets and as exponentials

Corrected

2) line 99 and 102 – references have not been converted in end-note

Corrected

3) Table 1. From where is the "Overall score" taken? Please provide number of reflections in highest resolution shell.

Done. See also the answer to Reviewer #1

4) Line 170 and throughout. The authors are sloppy in providing pdb codes. It should be 5A6I and not 56AI (does not exist) and 1GKO and not 1GK0. These errors should be corrected throughout the paper.

Thanks to the reviewer for noticing the mistake

5) Line 182. It looks like the authors claim that the main chain O oxygens of Glu117 are positioned 2.8 Å from each other. This is impossible. Please provide the correct names of the side chain oxygen atoms.

Atom labels have been corrected

6) Line 187. Please remove “for all subunits”.

This part has been removed

7) Figure 1. Please change A, B, A' and B' to A, A', A'' and A''' . There are no A and B chains in this structure.

We agree that all subunits of the tetramer are identical, i.e. they are all A chains, but in the crystal where a dimer is present in the a.u. the two monomers are conventionally labelled A and B, whilst when a tetramer is present in the a.u. the four chains are labeled A, B, C and D. This is necessary in order to distinguish monomers in the crystal. A note has been added in Fig. 1 caption.

8) Table 2 should be removed. It is likely that one of the Glu side chain is protonated at pH 7. But that does not mean that the pKa is 13!

Table 2 has been removed

9) Figure 2 – include that the superposition is based on monomer A

Done

10) Line 261 change to A-C and B-D. Coordinates 1GKO has a tetramer in the AU.

A comment was added in the text.

11) Table 5 line 199: which ligand?

Residues marked in red are the ones that make up the Halogen Binding Pocket, so they interact with ligands as defined in reference [33]. THR 118 and VAL 121 are not within the Halogen binding pocket, but they interact with T4 ligand.
